The Meteoritical Society

Meteoritics & Planetary Science 42, Nr 4/5, 513–540 (2007)
Abstract available online at http://meteoritics.org

Petrography, geochemistry, and alteration of country rocks from the Bosumtwi impact structure, Ghana

Forson KARIKARI[1*], Ludovic FERRIÈRE[1], Christian KOEBERL[1], Wolf Uwe REIMOLD[2], and Dieter MADER[1]

[1]Center for Earth Sciences, University of Vienna, Althanstrasse 14, A-1090 Vienna, Austria
[2]Museum of Natural History (Mineralogy), Humboldt University, Invalidenstrasse 43, D-10115 Berlin, Germany
[*]Corresponding author. E-mail: a0549738@unet.univie.ac.at

(Received 27 October 2006; revision accepted 18 January 2007)

Abstract–Samples of the country rocks that likely constituted the target rocks at the 1.07 Myr old Bosumtwi impact structure in Ghana, West Africa, collected outside of the crater rim in the northern and southern parts of the structure, were studied for their petrographic characteristics and analyzed for their major- and trace-element compositions. The country rocks, mainly meta-graywacke, shale, and phyllite of the Early Proterozoic Birimian Supergroup and some granites of similar age, are characterized by two generations of alteration. A pre-impact hydrothermal alteration, often along shear zones, is characterized by new growth of secondary minerals, such as chlorite, sericite, sulfides, and quartz, or replacement of some primary minerals, such as plagioclase and biotite, by secondary sericite and chlorite. A late, argillic alteration, mostly associated with the suevites, is characterized by alteration of the melt/glass clasts in the groundmass of suevites to phyllosilicates. Suevite, which occurs in restricted locations to the north and to the south-southwest of the crater rim, contains melt fragments, diaplectic quartz glass, ballen quartz, and clasts derived from the full variety of target rocks. No planar deformation features (PDFs) in quartz were found in the country rock samples, and only a few quartz grains in the suevite samples show PDFs, and in rare cases two sets of PDFs. Based on a total alkali element-silica (TAS) plot, the Bosumtwi granites have tonalitic to quartz-dioritic compositions. The Nb versus Y and Ta versus Yb discrimination plots show that these granites are of volcanic-arc tectonic provenance. Provenance studies of the metasedimentary rocks at the Bosumtwi crater have also indicated that the metasediments are volcanic-arc related. Compared to the average siderophile element contents of the upper continental crust, both country rocks and impact breccias of the Bosumtwi structure show elevated siderophile element contents. This, however, does not indicate the presence of an extraterrestrial component in Bosumtwi suevite, because the Birimian country rocks also have elevated siderophile element contents, which is thought to result from regional hydrothermal alteration that is also related to widespread sulfide and gold mineralization.

INTRODUCTION

The Bosumtwi crater in Ghana, West Africa, is centered at 06°30′N, 01°25′W. The 1.07 Myr old impact structure (Koeberl et al. 1997) is situated in the Ashanti region, about 32 km east of Kumasi, the regional capital. The Bosumtwi impact structure is arguably the youngest and best-preserved terrestrial impact structure larger than 6 km in diameter (Scholz et al. 2002; Earth Impact Database 2006). The crater has a pronounced rim, with a rim-to-rim diameter of about 10.5 km. The structure forms a hydrologically closed basin and is almost completely filled by Lake Bosumtwi (8.5 kilometers in diameter). The lake has a maximum depth of about 80 m and the crater rim rises about 250–300 m above the lake level. The area forms part of a tropical rain forest environment with warm climate, high rainfall, and high organic activity. Chemical weathering is intense, leading to the formation of locally thick lateritic soils.

Studies over the past 50 years have confirmed that the Bosumtwi crater structure was formed by meteorite impact. This is indicated by outcrops of suevitic breccia around the crater (Chao 1968; Jones et al. 1981), samples of which have been shown to contain the high-pressure quartz modification coesite (Littler et al. 1961), as well as Ni-rich iron spherules and baddeleyite in vesicular glass (El Goresy 1966; El Goresy et al. 1968). In addition, Koeberl et al. (1998) described shock-

characteristic planar deformation features (PDFs) in quartz from suevitic breccia (see also several papers in this issue).

The Bosumtwi impact structure is also the likely source crater for the Ivory Coast tektites (e.g., Gentner et al. 1964; Jones 1985; Koeberl et al. 1997, 1998). This correlation is mainly based on similarities in geochemical and isotopic compositions of target rocks and tektites, as well as similarities in the ages of the impact melt from suevites and of the Ivory Coast tektites. Boamah and Koeberl (2003) carried out detailed petrographic and geochemical studies on suevites from shallow drill cores obtained to the north of the crater. Results of structural and geological mapping of the Bosumtwi crater rim were reported by Reimold et al. (1998). Geochemical signatures of soils from north of the crater and their relationship to airborne radiometric geophysical data were discussed by Boamah and Koeberl (2002).

Various geophysical studies of the Bosumtwi structure have been carried out (Pesonen et al. 1998; Karp et al. 2002; Scholz et al. 2002). Koeberl and Reimold (2005) published an updated and revised geological map of the Bosumtwi structure and environs, with explanations containing more detail about the impact structure. The most recent research on the crater was a multinational drilling project by the International Continental Scientific Drilling Program (ICDP) during the second half of 2004, when 16 continuous cores of both lake sediments (14) and impactites (2) were obtained for paleoenvironmental and impact-cratering studies (papers in this issue), respectively.

Here we report the petrographic and geochemical characteristics of the main country rock types that likely constituted the target rocks at Bosumtwi and of suevites at the Bosumtwi impact structure, and discuss their pre- and post-impact alteration.

GEOLOGICAL SETTING

The Bosumtwi impact structure was excavated in rocks of the Early Proterozoic Birimian Supergroup (Jones at al. 1981). These rocks crop out extensively in Ghana, Ivory Coast, Burkina Faso, and Mali. The Birimian Supergroup consists of two major units: one unit composed dominantly of metamorphosed sedimentary rocks and the other unit mostly represented by bimodal, although largely tholeiitic, volcanics now altered and metamorphosed to greenstones. These greenstones initially comprised mainly basalts and andesites that have now been metamorphosed to hornblende-actinolite schist, calcite-chlorite schist, mica schist, and amphibolites. The metasedimentary unit comprises volcaniclastic rocks, turbidite-related wackes, argillitic rocks, and chemical sediments (Leube et al. 1990) now metamorphosed into meta-graywackes, phyllites, schists, and shales. The volcanic activity and sedimentation were submarine, according to Woodfield (1966), with evidence provided by the interfingering of, and lateral variation between, metavolcanics and metasediments, and the appearance of relict pillow structures in the metavolcanics.

Traditionally, in Ghana the metasedimentary unit was considered older than the metavolcanic unit (Junner 1937; Woodfield 1966; Moon and Mason 1967). This, however, was in contrast to the view held in the neighboring francophone countries (Hirdes et al. 1996). Recent studies have shown that the two units were formed contemporaneously (e.g., Leube et al. 1990). On the basis of Sm-Nd isochron and model ages, Taylor et al. (1992) constrained the age of Birimian supracrustal rocks of western Ghana to between 2.0 and 2.3 Gyr. Feybesse et al. (2006) placed somewhat tighter constraints on the age of these rocks, around 2.10 to 2.15 Gyr.

Two types of granitoid intrusions into the volcanic package and the basin sediments occur, which are referred to as the Belt (Dixcove) granitoids and the Basin (Cape Coast and Winneba) granitoids, respectively (Wright et al. 1985). According to Wright et al. (1985), the Belt-type granitoids are generally discordant to regional structures, often unfoliated, and of predominant dioritic to monzonitic composition, whereas the Basin-type granitoids are generally concordant to regional structures, often foliated, and of predominant granodioritic composition. Hirdes et al. (1992) characterized the Belt-type granitoids as a) small- to medium-sized plutons mainly restricted to the Birimian volcanic terrane, b) seldom foliated (except for local intense shearing) with no compositional banding, c) metaluminous, d) typically dioritic to granodioritic in composition, e) higher in Na_2O and CaO contents than the Basin-type granitoids, f) displaying pronounced retrograde alteration, g) containing similar geochemical characteristics as the metavolcanics in the belt for some elements, and h) bounded by contact aureoles of a few tens of meters maximum width. The Basin-type granitoids, on the other hand, were characterized as a) large batholiths restricted to Birimian sedimentary basins, b) having a foliation with compositional banding ubiquitous and pronounced, c) peraluminous, d) typically granodioritic in composition, e) higher in K_2O and Rb contents than the Belt-type granitoids, f) showing little mineral alteration, g) displaying no evidence for geochemical similarity to the metavolcanics in the belts, and h) having extensive contact-metamorphic aureoles. On the basis of U-Pb zircon and monazite dating, Hirdes et al. (1992) determined the age of the Belt-type granitoids in the Ashanti belt to be about 2175 Myr and the age of the Kumasi Basin-type granitoids at about 2116 Myr.

The majority of Birimian gold deposits and occurrences in Ghana is located at or along the boundaries between the metasediment units and five Birimian volcanic belts. The gold mineralization is associated with shear zones and extensive hydrothermal alteration (Wright et al. 1985; Melcher and Stumpfl 1994; Oberthür et al. 1994; Feybesse et al. 2006). Appiah (1991) reported formation of pyrite, arsenopyrite, sericite, chlorite, quartz, and carbonates both in

the wall rocks and quartz reefs. Melcher and Stumpfl (1994) also described hydrothermal alteration of the wall rock to gold reefs, involving chlorite, muscovite, graphite, carbonates, epidote, quartz (silicification), and sericite. Mineralogical and geochemical changes associated with alteration in Birimian rocks were also described by Pelig-Ba et al. (2004). The exact timing of hydrothermal alteration and gold mineralization is still not known (Dzigbodi-Adjimah 1993; Oberthür et al. 1994). On the basis of Pb isotope compositions of galena and bournonite from gold-quartz veins, Oberthür et al. (1994) obtained model ages between 2122 and 1940 Myr. The Pb isotope compositions of arsenopyrite from sulfide ores in Birimian host rocks gave an isochron age of 2224 ± 20 Myr. Fine-grained muscovite (sericite) from Birimian sediment-hosted ore yielded K-Ar ages ranging from 1867 ± 42 to 1893 ± 43 Myr. In view of the uncertainties inherent to these data, Oberthür et al. (1994) established an upper age limit of 2132 Myr, which is relatively well constrained, and an uncertain lower age limit of 2100 Myr. In their Birimian evolution model, Feybesse et al. (2006) suggested the gold mineralization was emplaced during the late stage of the Eburnean event (Eburnean D2 tectonism between 2095–1980 Myr) and was associated with NE-SW ductile transcurrent faults.

The Bosumtwi impact structure is located within Birimian rocks and near several localized granite intrusions. The geology of the Bosumtwi impact structure and environs has been described by several authors (e.g., Junner 1937; Woodfield 1966; Moon and Mason 1967; Jones et al. 1981; Reimold et al. 1998; Koeberl and Reimold 2005). The crater structure also occurs in the proximity of a contact between metasedimentary and metavolcanic units of the Ashanti belt (Fig. 1). The corridor along the flanks of this contact elsewhere in the Ashanti belt is well known for the occurrence of shear zones and associated gold mineralization (e.g., Leube et al. 1990; Milesi et al. 1992; Melcher and Stumpfl 1994; Yao and Robb 2000).

The Birimian rocks, in which the crater was excavated, comprise shales, phyllites, schists, meta-graywackes, and granitoids (e.g., Junner 1937). The Birimian metavolcanic rocks extend to the southeast of the crater. On the west and northwest sides of the lake, phyllites, shales, meta-graywackes, and quartzites are exposed, whereas the other parts show mainly exposures of phyllites. Extensive graphitic phyllite and shale occur in the southern sector occur. The metasedimentary rocks are intruded by microgranite dikes up to 60 m wide. In the northeast sector of the crater, rocks of the Pepiakese intrusion are found, comprising a variety of rock types ranging from hornblende- to biotite-muscovite granite (Jones 1985) and diorite (Koeberl et al. 1998). The Pepiakese intrusion is thought to be related to the Kumasi (Basin-type) granitoids.

Impact breccias are widely exposed at and around the crater. These breccias are monomict lithic breccia (autochthonous) and polymict lithic breccia (allochthonous) from the various target rocks, as well as suevites (polymict impact melt- or glass-bearing breccias), which occur to the north and south of the crater. The suevite contains target rock fragments representative of all stages of shock metamorphism, as well as vitreous and devitrified impact glasses (Reimold et al. 1998; Boamah 2001).

SAMPLES AND EXPERIMENTAL METHODS

A suite of samples, previously collected by two authors (C. K. and W. U. R.) during fieldwork in 1997 in the direct vicinity of the crater and on the crater rim, was selected for both petrographic and geochemical studies. Thirty-one thin sections (representing 4 shale/phyllite, 4 meta-graywacke, 8 granite, a siltstone, a quartz-rich schist, 3 suevite, and 10 melt/glass fragments from suevite samples) were prepared and investigated by optical microscopy. For each sample, the rock type, minerals present, and shock effects were studied (Table 1).

For geochemical studies, 36 samples (6 shale/phyllite, 3 meta-graywacke, 9 granite, an arkose, a siltstone, a quartz-rich schist, a quartz vein, 8 suevite and 6 melt/glass fragments from suevite samples) were crushed in polyethylene wrappers and powdered in a mechanical agate mill for bulk chemical analysis.

The contents of major elements (Si, Ti, Al, Mn, Mg, Ca, and P) and trace elements (V, Cu, Zn, Y, and Nb) of 26 samples were determined by standard X-ray fluorescence (XRF) spectrometry at the University of the Witwatersrand, Johannesburg, South Africa. Reimold et al. (1994) described the procedures, precision, and accuracy of the XRF analytical method. Ten other samples (LB-2, LB-5, LB-9, LB-11, LB-13, LB-24, LB-33, LB-34, LB-40, and LB-46) were analyzed by XRF spectrometry at the Department of Geological Sciences, University of Vienna, Austria. However, due to inadequate sample amounts available, the trace-element contents of LB-9 and LB-13 could not be determined by XRF (see Tables 2 and 3).

The contents of major elements (Fe, Na, and K) and trace elements (Sc, Cr, Co, Ni, As, Se, Br, Rb, Sr, Zr, Sb, Cs, Ba, Hf, Ta, Th, and U), including the rare earth elements (REE), were determined for all 36 samples by instrumental neutron activation analysis (INAA) at the Department of Geological Sciences, University of Vienna, Austria. For details of the INAA method, including precision and accuracy, see Koeberl (1993).

RESULTS

Petrography

The sample locations, rock types, and petrographic observations are summarized in Table 1. Microphotographs of

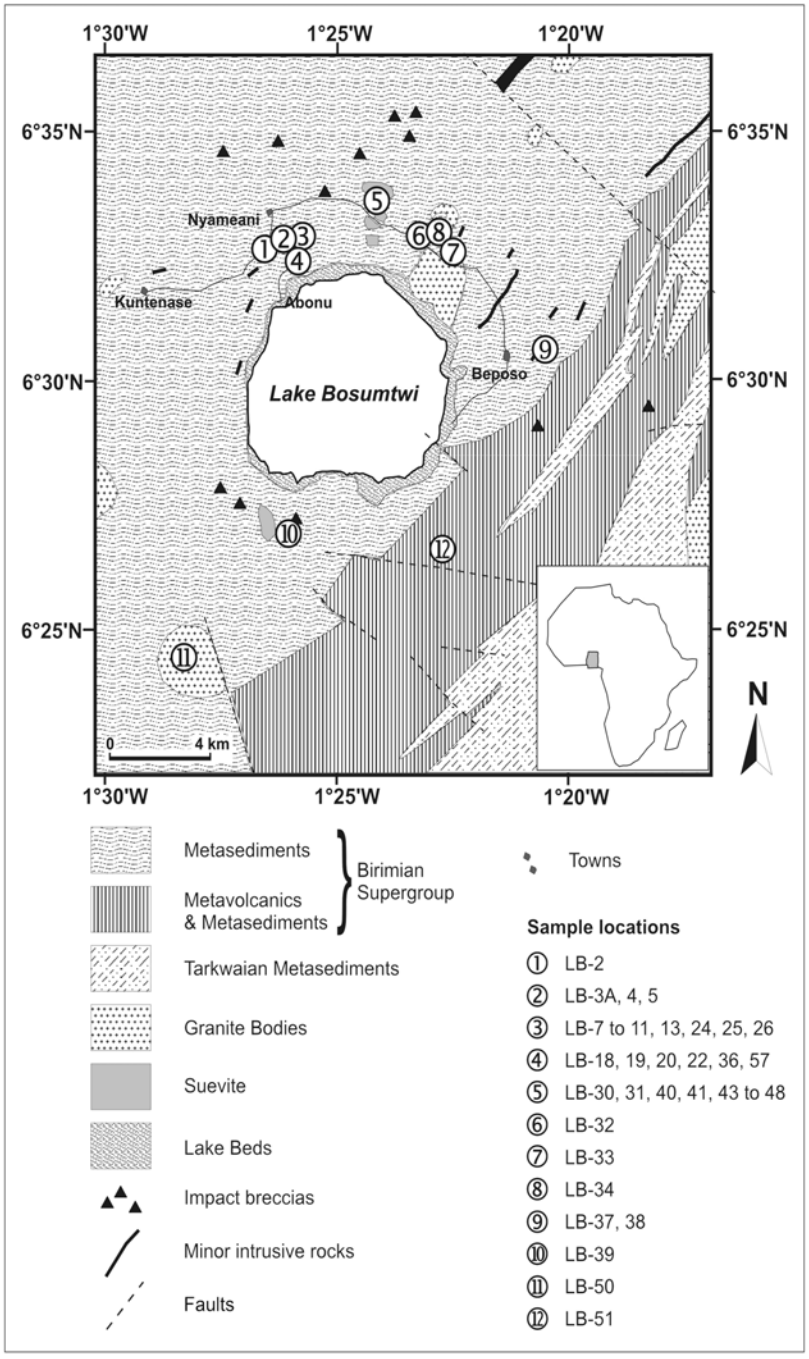

Fig. 1. A geological map of the area of the Bosumtwi impact structure in Ghana (inset). Modified after Jones et al. (1981) and Reimold et al. (1998). The locations of sampling sites are also shown.

some typical alteration and other characteristics of the country rock and suevite samples are shown in Figs. 2–8. A generalized description of the main country rock types and the suevites is given below.

Shale

In hand specimen two types of shale, differing in color and appearance, can be distinguished: a) banded shale, which is a soft, highly argillaceous rock consisting of alternating, very thin beds of light gray, dark gray, or black color, and b) graphitic shale, which is also a soft but dull black, argillaceous rock that stains the fingers when handled. There is minor disseminated sulfide in some of the shale samples. The thin sections show quartz, feldspar, iron oxides, opaque minerals (sulfides), and very fine-grained, optically unidentifiable phyllosilicates (Fig. 2a). Some shale samples

Table 1. Petrographic description of rock samples from the Bosumtwi impact structure collected in 1997.

Sample no.	Location	Rock type	Petrographic description
LB-2	6°32.8′N 1°26.4′W	Siltstone	Massive, very fine-grained, greenish gray siltstone with shear fabric; quartz dominant, rich in biotite (locally altered to chlorite), some feldspar, muscovite, and large nodules of opaque minerals; a few veinlets of Fe oxides occur; no evidence of shock.
LB-3A	6°33.05′N 1°25.9′W	Quartz-rich schist	Quartzite bands (about 2–3 mm thick) with thin intercalated biotite-rich bands (up to 1 mm); quartz is well sutured and frequently displays undulatory extinction; some fine-grained biotite is partially aligned parallel to the schistosity, partially discordant, and much biotite is deformed (kink banding); no characteristic evidence of shock.
LB-5	6°33.05′N 1°25.9′W	Shale	Very fine-grained, gray-black shale with some even darker (carbon-rich?) bands; composed of quartz, feldspar, and Fe oxides; a few thin veinlets of quartz cross-cut the section; no evidence of shock.
LB-7	6°33.15′N 1°25.75′W	Meta-graywacke (biotite rich)	Medium-grained, mylonitized, meta-graywacke; composed of quartz (47 vol%), plagioclase (6 vol%), K-feldspar (9 vol%), biotite (7 vol%), and opaque minerals and other traces (2 vol%); large biotite grains are partially oxidized; fine-grained chlorite grains appear unaltered; feldspar is partially altered to sericite; no evidence of shock. Matrix (mainly biotite, chlorite, and sericite) is 29 vol%.
LB-8	6°33.12′N 1°25.63′W	Meta-graywacke	Medium-grained, gray meta-graywacke; composed of quartz (39 vol%), K-feldspar (6 vol%), plagioclase (4 vol%), sericite, chlorite, muscovite, and opaque minerals (1 vol%); most of the feldspar is altered to sericite, and biotite is completely altered to chlorite. Matrix (mainly sericite, chlorite and quartz) is 40 vol%; no evidence of shock.
LB-10	6°33.06′N 1°25.6′W	Microgranite	Altered fine- to medium-grained microgranite; composed of plagioclase (26 vol%), quartz (24 vol%), K-feldspar (14 vol%), biotite (13 vol%), muscovite (12 vol%), Fe oxides (9 vol%), and accessory minerals (2 vol%); biotite grains are mostly oxidized; no evidence of shock.
LB-11	6°33.06′N 1°25.6′W	Mylonitic shale	Fine-grained, dark gray mylonitic shale; composed of quartz, phyllosilicates, feldspar, and opaque minerals; some wide quartz ribbons; no evidence of shock.
LB-18	6°32.7′N 1°25.7′W	Microgranite	Fine- to medium-grained, slightly sheared microgranite; consists of quartz (40 vol%), plagioclase (20 vol%), K-feldspar (10 vol%), biotite (10 vol%), muscovite/sericite (13 vol%), chlorite (6 vol%), and accessory minerals (mainly sphene) (1 vol%); most of the biotite is oxidized and occurs in "clusters;" some granophyric intergrowths of quartz in K-feldspar; no evidence of shock.
LB-19A	6°32.7′N 1°25.7′W	Granite	Altered medium-grained granite; consists of quartz (27 vol%), K-feldspar (22 vol%), plagioclase (11 vol%), biotite (5 vol%), muscovite (5 vol%), chlorite (27 vol%), Fe oxides and accessory minerals (e.g., sphene) (3 vol%); granophyric intergrowth of quartz and K-feldspar is abundant; nice spherulites of feldspar; most of the biotite is altered; micro-fractures partially filled with Fe oxides cross-cut the section; no evidence of shock.
LB-19B	6°32.7′N 1°25.7′W	Meta-graywacke	Altered medium-grained, sheared, meta-graywacke (biotite-rich, similar to sample LB-7); composed of quartz (36 vol%), plagioclase (7 vol%), K-feldspar (9 vol%), biotite (5 vol%), sericite, and opaque minerals (mainly Fe oxides) (3 vol%); some biotite grains are partially oxidized; some feldspar grains are partially altered to sericite; no evidence of shock. Matrix (mainly sericite, quartz, chert, and chlorite) amounts to 42 vol%.
LB-24	6°33.0′N 1°25.6′W	Granite	Medium-grained granite (very few oxides in this sample compared to LB-25 and very little granophyric intergrowth; no spherulites observed); consists of plagioclase (42 vol%), K-feldspar (30 vol%), quartz (8 vol%), biotite (some completely oxidized/ altered to chlorite) (13 vol%), muscovite (5 vol%), and Fe oxide and accessory minerals (2 vol%); most feldspar is altered to sericite; no evidence of shock.
LB-25	6°33.0′N 1°25.6′W	Granite	Altered medium-grained granite (similar to LB-19A but with more oxides); consists of quartz (35 vol%), K-feldspar (15 vol%), plagioclase (10 vol%), secondary phyllosilicate (25 vol%), biotite completely altered to chlorite (5 vol%), and Fe oxide (10 vol%); granophyric intergrowth of quartz; K-feldspar is abundant; some spherulites of feldspar; no evidence of shock.
LB-26	6°33.0′N 1°25.6′W	Granite	Altered fine- to medium-grained granite; composed of quartz (38 vol%), K-feldspar (10 vol%), plagioclase (5 vol%), biotite (completely altered to chlorite, 10 vol%), Fe oxides (4 vol%), and sericite (37 vol%); some well-developed spherulites of feldspar; granophyric intergrowth of quartz and K-feldspar occurs mostly at the edges of the spherulites; no evidence of shock.
LB-32	6°33.1′N 1°22.9′W	Mylonitic shale/ phyllite	Very fine- to fine-grained mylonitic shale/ phyllite, dark gray in color (sample locally similar to LB-11); composed of quartz, phyllosilicates (biotite identified; other phyllosilicates optically not identifiable), feldspar, and opaque minerals; thin quartz veinlets cross-cut the section; no evidence of shock.
LB-33	6°32.90′N 1°22.28′W	Meta-graywacke	Medium-grained meta-graywacke (similar to LB-8 but matrix poor); composed of quartz (64 vol%), K-feldspar (12 vol%), plagioclase (9 vol%), biotite (mostly oxidized) (1 vol%), opaque minerals (1 vol%), and accessory minerals (zircon, sphene, epidote) (2 vol%); a few feldspar grains are partially altered to sericite; some quartz grains show undulatory extinction. Matrix (mainly sericite, quartz, and chlorite) amounts to 11 vol%; no evidence of shock.

Table 1. *Continued.* Petrographic description of rock samples from the Bosumtwi impact structure collected in 1997.

Sample no.	Location	Rock type	Petrographic description
LB-34	6°33.13′N 1°22.64′W	Granite	Granite composed mainly of quartz (38 vol%), plagioclase (29 vol%), K-feldspar (15 vol%), biotite (5 vol%), sericite (12 vol%), and traces of Fe oxides and other opaque minerals (1 vol%); very large biotite grains (partially oxidized); feldspar is partially altered to sericite; no evidence of shock.
LB-38	6°30.79′N 1°20.52′W	Granite	Coarse-grained granite, muscovite-rich; composed of quartz, K-feldspar, plagioclase, muscovite, sericite, chlorite, and opaque minerals; feldspar is intensely altered to sericite; no evidence of shock.
LB-39a	6°26.98′N 1°25.88′W	Suevite	Suevite (brownish in color) with angular to subrounded lithic clasts (up to 2 cm size) set into a clastic matrix (40 vol%); clasts include graphitic shale (13 vol%), phyllite (7 vol%), meta-graywacke (13 vol%), microgranite (2 vol%), quartz and quartzitic grains (10 vol%), chert (4 vol%), melt (altered and/or recrystallized) fragments and diaplectic quartz glass (together 11 vol%). A few quartz grains show PDFs; some clasts and matrix are altered (brownish oxides, chlorite, and other phyllosilicates).
LB-39c	6°26.98′N 1°25.88′W	Suevite	Suevite (brownish in color, similar to sample LB-39a) with angular to subrounded clasts (up to 1.5 cm) in a clastic matrix; clasts include phyllite, meta-graywacke, microgranite, glass/melt (mostly vesicular and fresh), diaplectic quartz glass, quartz, quartzite, and feldspar. A few quartz grains show PDFs (up to 2 sets); some clasts and matrix are altered to phyllosillicates (argillic alteration).
LB-40	6°33.88′N 1°23.88′W	Large melt fragment from suevite	Large, gray melt fragment from suevite (gray) that consists of melt matrix and melted or vitrified clasts (88 vol%); very few clasts are unmelted; unshocked meta-graywacke clasts (9 vol%); few quartz (3 vol%) and feldspar clasts (<1 vol%); melt/glass (some fragments very vesicular and others partially recrystallized), diaplectic quartz, and ballen quartz are dominant, are dominant, and a few vitrified metasediment clasts are present as well.
LB-43	6°33.88′N 1°23.88′W	Suevite	Suevite (brownish in color, very similar to sample LB-39a) with some angular to subrounded clasts in a clastic matrix (42 vol%); clast population includes shale (15 vol%), microgranite (5 vol%), vitrified phyllite (6 vol%), melt/glass (mostly fresh vesicular glass, diaplectic quartz glass, some altered melt) (12 vol%), meta-graywacke (13 vol%), and quartz and quartzitic grains (7 vol%); some clasts and matrix are altered (brownish oxides, chlorite); a few quartz grains with PDFs (up to 2 sets).
LB-44A	6°33.88′N 1°23.88′W	Melt fragment from suevite	Melt clast from suevite, highly vesicular and very clast-poor; clast population includes diaplectic quartz glass, ballen quartz, unshocked quartz, and one vitrified meta-graywacke.
LB-44B	6°33.88′N 1°23.88′W	Melt clast from suevite	Melt clast from suevite (similar to sample LB-44A) with rounded, 2 cm wide ballen quartz inclusion.
LB-45	6°33.88′N 1°23.88′W	Melt clast from suevite	Melt clast from suevite, highly vesicular and very clast-poor (similar to sample LB-44A); clast population includes diaplectic quartz glass, ballen quartz, vitrified meta-graywacke, and unshocked quartz.
LB-45A	6°33.88′N 1°23.88′W	Melt clast from suevite	Melt clast from suevite, highly vesicular and very clast-poor (<5 vol%; similar to sample LB-45); clast population includes diaplectic quartz glass, ballen quartz, and unshocked quartz.
LB-45B	6°33.88′N 1°23.88′W	Melt fragment from suevite	Melt fragment from bulk suevite, gray in color, similar to sample LB-47A; consists of melt matrix and melted or vitrified clasts (only a few quartz, meta-graywacke, quartzite, and feldspar clasts are unmelted); melt/glass (some highly vesicular, others partially recrystallized), diaplectic quartz, and ballen quartz, and a few vitrified metasediment (mainly graywacke) clasts are present.
LB-46	6°33.88′N 1°23.88′W	Melt fragment from suevite	Melt fragment sample, gray in color, similar to sample LB-45B.
LB-47A	6°33.88′N 1°23.88′W	Melt fragment from suevite	Melt fragment from suevite (gray in color, very similar to sample LB-40) that consists of melt matrix and melted or vitrified clasts (few quartz, meta-graywacke, and quartzite clasts are unmelted or unvitrified); melt/glass (some fragments are very vesicular and/or with flow structure, others are partially recrystallized), diaplectic quartz, and ballen quartz are dominant, but also some vitrified metasediment clasts.
LB-47B	6°33.88′N 1°23.88′W	Melt fragment from suevite	Melt fragment from suevite (gray in color, very similar to sample LB-47A) that consists of melt matrix and melted or vitrified clasts (few quartzite, quartz, and feldspar are unmelted or unvitrified); melt/glass (with well-developed flow structure, some fragments are highly vesicular, others are partially recrystallized), diaplectic quartz, and ballen quartz are dominant.
LB-48	6°33.88′N 1°23.88′W	Melt clast from suevite	Large, >4 cm in diameter melt clast in suevite (light gray in color); well-developed flow structures are visible; some parts of the clast are highly vesicular, others are partially recrystallized; few unmelted or unvitrified quartz and quartzite clasts are also preserved inside the melt fragment; diaplectic quartz and ballen quartz are also present.
LB-51	6°26.74′N 1°22.62′W	Graphitic shale	Well-laminated, fine-grained graphitic shale (black gray in color); composed mainly of quartz, optically unidentifiable phyllosilicates, and carbon (graphite?); local development of crenulation cleavage; no trace of shock deformation.

Table 2. Major and trace element composition of country rocks from the Bosumtwi impact structure.

	Shale/phyllite						Meta-graywacke			Siltstone	Arkose	Quartz-rich schist	Quartz (vein?)
	Graphitic shale	Shale											
	LB-51	LB-5	LB-11	LB-32	LB-37	LB-13[a]	LB-9[a]	LB-22	LB-33	LB-2	LB-20	LB-3A	LB-4
SiO_2	71.3	58.1	63.5	66.6	59.4	65.1	71.0	67.3	74.7	66.1	69.2	87.8	100.4
TiO_2	0.81	0.13	0.64	0.72	0.81	0.63	0.43	0.59	0.34	0.58	0.53	0.27	0.10
Al_2O_3	9.70	14.4	17.2	15.9	18.0	16.8	12.6	15.6	10.8	16.0	14.4	4.51	<0.01
Fe_2O_3	7.45	6.83	6.50	6.51	10.5	5.52	4.55	5.75	3.37	5.89	4.36	3.05	0.40
MnO	0.07	0.06	0.05	0.03	0.13	0.03	0.12	0.03	0.05	0.04	0.05	0.04	0.01
MgO	3.20	1.84	2.22	2.14	0.44	2.23	1.16	1.87	1.06	1.95	2.03	0.87	<0.01
CaO	<0.01	0.99	0.44	0.14	<0.01	0.44	1.01	0.88	0.78	0.72	0.91	0.19	0.01
Na_2O	0.21	1.49	2.03	0.35	1.52	2.20	3.22	3.11	3.57	2.70	4.39	0.73	0.02
K_2O	0.56	2.54	2.74	2.75	2.50	2.12	0.90	1.62	0.37	2.75	0.69	0.58	0.01
P_2O_5	0.05	0.47	0.13	0.07	0.12	0.13	0.12	0.09	0.04	0.18	0.11	0.03	<0.01
LoI	6.91	12.4	4.08	5.70	5.33	4.23	3.96	3.41	1.37	3.34	2.95	2.15	<0.01
Total	100.3	99.24	99.47	101.0	98.69	99.41	99.08	100.3	96.39	100.2	99.63	100.2	100.9
SiO_2/Al_2O_3	7.35	4.04	3.70	4.18	3.30	3.88	5.62	4.31	6.93	4.14	4.79	19.5	
K_2O/Na_2O	2.64	1.71	1.35	7.82	1.64	0.97	0.28	0.52	0.10	1.02	0.16	0.78	0.42
Sc	15.7	23.6	19.2	16.6	20.1	16.5	9.23	12.2	6.74	14.3	11.5	6.00	0.08
V	126	95	130	124	131			111	77	98	115	52	<5
Cr	118	95.7	85.5	162	94.0	80.0	46.5	79.0	45.5	81.6	71.4	47.3	5.40
Co	15.6	12.3	14.6	24.0	31.2	4.29	21.4	13.1	10.7	12.2	9.33	10.6	0.19
Ni	256	70	52	88	63	23	37	35	17	43	34	20	3
Cu	114	43	34	18	43			13	24	95	<2	<2	<2
Zn	103	66	74	105	153			63	49	84	38	50	<9
As	5.24	1.06	2.31	3.39	65.8	3.87	2.63	0.41	1.13	0.12	3.09	0.69	0.72
Se	0.2	12.1	1.8	0.2	0.2	1.5	1.5	<1.4	1.5	2.4	2.0	<1.2	0.2
Rb	22.3	54.1	94.5	91.0	92.1	80.8	33.0	61.7	16.5	76.7	27.1	25.9	0.83
Sr	65.2	200	206	103	194	320	302	327	282	313	469	105	15.4
Y	33	64	19	5	22			11	14	23	11	5	<3
Zr	181	111	121	123	164	92.7	135	116	132	183	151	37.5	4.93
Nb	10	6	9	10	12			9	8	10	8	7	5
Sb	4.02	0.15	0.11	0.30	1.38	0.16	0.13	0.14	0.10	0.16	0.17	0.11	0.10
Cs	0.81	1.84	3.66	2.94	2.74	3.13	1.57	2.59	0.92	3.24	1.47	1.35	0.06
Ba	344	1170	836	587	639	498	363	661	146	1102	189	199	29.5
La	17.3	110	5.28	2.03	27.3	2.34	3.50	9.94	23.8	12.6	16.0	5.20	0.09
Ce	28.3	223	22.8	4.04	60.6	7.44	13.7	23.27	46.8	25.6	22.9	16.8	0.16
Nd	17.0	116	7.44	2.15	25.2	4.14	5.93	11.97	19.0	13.4	10.7	5.15	0.27
Sm	4.32	23.7	1.52	0.52	5.05	0.90	1.33	2.54	3.30	3.16	2.35	1.15	0.02
Eu	1.16	5.63	0.50	0.17	1.36	0.29	0.30	0.76	1.03	0.94	0.96	0.35	0.01
Gd	4.58	19.2	1.66	0.80	4.35	1.11	1.30	2.30	2.93	2.60	2.62	1.06	0.56
Tb	0.96	2.55	0.34	0.14	0.75	0.18	0.30	0.36	0.37	0.48	0.39	0.17	0.02
Tm	0.47	0.74	0.27	0.16	0.40	0.16	0.14	0.22	0.17	0.29	0.22	0.10	0.06
Yb	3.22	4.96	1.93	1.28	2.38	1.30	1.01	1.57	1.01	2.29	1.53	0.70	0.05
Lu	0.54	0.67	0.28	0.20	0.38	0.21	0.16	0.26	0.17	0.33	0.22	0.10	0.00

Table 2. *Continued.* Major and trace element composition of country rocks from the Bosumtwi impact structure.

	Shale/phyllite						Meta-graywacke			Siltstone	Arkose	Quartz-rich schist	Quartz (vein?)
	Graphitic shale	Shale											
	LB-51	LB-5	LB-11	LB-32	LB-37	LB-13[a]	LB-9[a]	LB-22	LB-33	LB-2	LB-20	LB-3A	LB-4
Hf	2.50	2.36	2.73	3.52	4.19	2.43	2.40	3.10	2.61	4.19	3.16	0.76	0.01
Ta	0.45	0.08	0.43	0.54	0.57	0.39	0.26	0.30	0.28	0.47	0.34	0.15	0.03
Au (ppb)	15	5.00	1.4	0.2	<1.2	1.5	1.6	<1.1	0.8	1.0	1.3	0.3	0.1
Th	2.87	2.44	3.22	3.76	4.64	2.63	1.79	3.08	3.32	3.22	3.06	1.00	0.02
U	2.53	6.20	1.58	1.41	2.72	1.12	0.53	0.59	0.78	0.63	0.63	0.39	0.02
CIA	91	67	71	81	78	78	61	65	58	65	60	67	
K/U	1842	3405	14,376	16,189	7634	15,683	14,154	22,995	3939	36,452	9193	12,390	3195
Th/U	1.14	0.39	2.03	2.67	1.71	2.34	3.40	5.26	4.28	5.13	4.89	2.59	1.30
La/Th	6.02	44.9	1.64	0.54	5.87	0.89	1.96	3.22	7.17	3.91	5.24	5.21	3.85
Zr/Hf	72.3	47.0	44.1	34.8	39.1	38.1	56.0	37.5	50.8	43.6	47.8	49.6	460
Hf/Ta	5.62	28.4	6.32	6.58	7.36	6.17	9.35	10.2	9.31	8.91	9.34	4.95	0.33
La_N/Yb_N	3.63	14.9	1.85	1.07	7.73	1.22	2.33	4.29	16.0	3.71	7.09	5.03	1.08
GdN/Yb_N	1.15	3.14	0.70	0.51	1.48	0.69	1.04	1.19	2.36	0.92	1.39	1.23	8.47
Eu/Eu*	0.80	0.81	0.95	0.80	0.89	0.87	0.69	0.96	1.01	1.00	1.18	0.97	0.37

[a]Sample not analyzed by XRF for trace elements (lack of material); blank spaces = not determined; N = chondrite-normalized (Taylor and McLennan 1985); chemical index of alteration (CIA) = $(Al_2O_3/[Al_2O_3 + CaO + Na_2O + K_2O]) \times 100$ in molecular proportions; $Eu/Eu^* = Eu_N/(Sm_N \times Gd_N)^{0.5}$.
Major elements in wt%, trace elements in ppm, except as noted; all Fe as Fe_2O_3.

Table 2. *Continued.* Major and trace element composition of target rocks from the Bosumtwi impact structure.

	Microgranite	Microgranite	Granite	Granite	Granite	Granite	Granite	Granite	Granite
	LB-10	LB-18	LB-24	LB-26	LB-34	LB-36	LB-38	LB-50	LB-57
SiO_2	62.8	65.6	67.2	61.3	74.3	66.4	71.4	68.4	63.6
TiO_2	0.69	0.62	0.45	0.60	0.13	0.67	0.99	0.58	0.52
Al_2O_3	17.6	15.0	16.4	14.4	14.9	16.9	17.3	15.1	14.9
Fe_2O_3	5.58	5.51	4.36	7.76	1.10	4.72	0.98	3.19	6.04
MnO	0.05	0.08	0.06	0.11	0.02	0.05	0.01	0.08	0.08
MgO	2.59	3.98	1.20	5.72	0.30	1.74	0.34	1.69	5.88
CaO	0.81	0.97	2.16	0.12	0.80	1.09	0.16	3.14	0.62
Na_2O	3.51	3.18	4.58	1.57	5.21	4.37	4.67	4.86	2.89
K_2O	1.46	0.85	0.82	1.20	2.25	1.63	1.81	2.57	0.93
P_2O_5	0.17	0.19	0.15	0.10	0.03	0.24	0.02	0.23	0.17
L.O.I	4.95	4.07	2.34	7.36	1.07	3.25	2.34	0.53	5.28
Total	100.1	100.1	99.74	100.3	100.0	101.0	100.1	100.3	100.9
SiO_2/Al_2O_3	3.57	4.36	4.09	4.26	4.99	3.92	4.12	4.54	4.27
K_2O/Na_2O	0.42	0.27	0.18	0.76	0.43	0.37	0.39	0.53	0.32
Sc	15.0	15.9	8.68	20.7	3.58	13.0	3.61	6.11	16.4
V	113	124	83	139	14	64	67	50	105
Cr	57.1	50.6	7.01	550	9.00	36.5	22.5	39.5	540
Co	13.1	17.9	9.43	24.0	0.98	9.13	5.63	8.67	23.0

Table 2. *Continued.* Major and trace element composition of target rocks from the Bosumtwi impact structure.

	Microgranite	Microgranite	Granite	Granite	Granite	Granite	Granite	Granite	Granite
	LB-10	LB-18	LB-24	LB-26	LB-34	LB-36	LB-38	LB-50	LB-57
Ni	34	20	19	124	9	18	13	27	135
Cu	<2	<2	19	<2	15	<2	<2	8	<2
Zn	78	70	57	96	35	59	25	69	78
As	13.2	0.93	1.36	3.56	2.60	0.95	4.86	5.73	1.14
Se	1.1	1.5	1.3	2.3	1.5	<1.3	0.4	<1.2	<1.8
Rb	46.7	46.0	29.4	45.7	50.5	59.7	60.9	79.6	19.4
Sr	202	390	488	157	256	361	566	1205	241
Y	10	11	13	13	13	18	11	13	10
Zr	173	155	130	105	78.2	131	232	247	105
Nb	10	8	7	8	9	9	20	10	8
Sb	0.36	0.25	0.22	0.12	0.14	0.31	<0.11	0.10	0.02
Cs	2.05	2.09	1.35	1.98	2.10	2.96	2.85	4.42	0.77
Ba	254	323	297	348	624	676	536	1420	168
La	7.61	27.5	10.4	21.7	13.1	19.4	23.8	71.2	16.0
Ce	18.5	56.6	24.3	43.2	23.3	36.0	50.3	127	32.2
Nd	6.17	28.9	10.7	20.3	11.3	23.0	27.6	61.7	16.9
Sm	1.15	4.95	2.30	3.94	1.70	4.25	5.19	10.3	3.61
Eu	0.32	1.33	0.87	1.12	0.50	1.26	1.40	2.77	1.12
Gd	1.75	3.40	2.17	3.26	1.50	3.55	3.40	6.13	3.00
Tb	0.32	0.47	0.40	0.52	0.25	0.63	0.39	0.68	0.41
Tm	0.19	0.21	0.17	0.27	0.17	0.26	0.11	0.17	0.18
Yb	1.47	1.33	1.05	1.89	1.16	2.11	0.65	0.90	1.02
Lu	0.27	0.19	0.14	0.24	0.15	0.33	0.06	0.14	0.15
Hf	6.72	2.77	2.36	2.50	2.28	3.29	5.57	4.91	2.36
Ta	1.07	0.29	0.24	0.24	0.50	0.29	1.30	0.41	0.20
Au (ppb)	0.5	0.7	1.5	0.0	1.2	<1.4	1.9	0.6	0.5
Th	4.36	5.06	1.48	2.11	2.55	2.76	3.61	8.37	2.21
U	1.60	0.93	0.65	1.02	1.38	0.72	1.40	2.72	0.68
CIA	67	65	57	78	54	61	64	48	68
K/U	7619	7622	10,569	9726	13,550	18,785	10,722	7859	11,422
Th/U	2.73	5.45	2.30	2.06	1.86	3.83	2.57	3.08	3.25
La/Th	1.74	5.45	7.00	10.3	5.13	7.04	6.59	8.50	7.24
Zr/Hf	25.7	55.8	55.2	42.0	34.3	39.9	41.7	50.4	44.4
Hf/Ta	6.26	9.59	9.94	10.6	4.55	11.4	4.30	12.0	11.7
La_N/Yb_N	3.50	14.0	6.66	7.76	7.62	6.22	24.9	53.4	10.6
Gd_N/Yb_N	0.97	2.07	1.67	1.40	1.05	1.37	4.27	5.52	2.39
Eu/Eu*	0.70	0.99	1.19	0.95	0.95	0.99	1.02	1.07	1.04

Major elements in wt%, trace elements in ppm, except as noted; All Fe as Fe_2O_3; blank spaces = not determined; N = chondrite-normalized (Taylor and McLennan 1985); chemical index of alteration (CIA) = $(Al_2O_3/[Al_2O_3 + CaO + Na_2O + K_2O]) \times 100$ in molecular proportions; $Eu/Eu^* = EuN/(Sm_N \times Gd_N)^{0.5}$.

Table 3. Major- and trace-element composition of suevites and melt/glass fragments from the Bosumtwi impact structure.

	Suevite								Melt/glass fragment					
	LB-30a	LB-30b	LB-31b	LB-31a-6[a]	LB-39a	LB-39c	LB-41	LB-43	LB-40	LB-44	LB-45	LB-46	LB-47	LB-48
SiO_2	63.3	53.1	60.2		59.3	62.8	63.0	72.9	65.8	63.3	64.3	68.1	67.4	61.3
TiO_2	0.66	0.79	0.82		0.75	0.71	0.66	0.50	0.67	0.67	0.67	0.56	0.58	0.75
Al_2O_3	15.4	21.1	19.0		17.8	15.4	17.2	12.3	17.3	16.7	16.4	15.6	15.8	16.5
Fe_2O_3	6.29	9.97	7.03	4.91	7.49	7.14	5.92	4.92	6.59	6.11	6.18	6.15	4.62	6.41
MnO	0.05	0.06	0.05		0.10	0.13	0.04	0.05	0.03	0.04	0.03	0.04	0.07	0.04
MgO	0.79	2.02	1.71		2.61	2.48	0.91	2.28	0.83	1.25	0.99	0.77	1.67	1.25
CaO	1.17	1.06	0.94		0.87	0.51	0.90	0.26	0.98	1.04	1.37	1.32	3.15	1.34
Na_2O	1.86	1.62	2.09	2.47	1.78	1.96	1.85	2.91	1.69	2.00	2.39	2.60	3.78	2.63
K_2O	1.34	3.10	2.52	1.88	1.93	1.73	1.11	1.68	1.77	1.69	1.38	1.65	2.63	1.78
P_2O_5	0.06	0.10	0.08		0.11	0.15	0.06	0.10	0.07	0.05	0.06	0.06	0.22	0.09
L.O.I	8.75	6.63	4.52		7.08	6.50	8.18	3.43	4.15	7.40	5.61	2.80	0.53	6.74
Total	99.67	99.60	98.91		99.78	99.46	99.87	101.2	99.92	100.3	99.36	99.61	100.4	98.79
SiO_2/Al_2O_3	4.11	2.51	3.17		3.34	4.09	3.66	5.94	3.81	3.78	3.92	4.37	4.27	3.71
K_2O/Na_2O	0.72	1.91	1.20	0.76	1.08	0.88	0.60	0.58	1.04	0.85	0.58	0.63	0.70	0.67
Sc	16.3	25.5	17.3	14.0	18.0	17.2	15.9	15.3	17.0	16.1	17.8	15.0	15.7	17.5
V	92	150	129		144	146	110	86	104	118	105	97	48	113
Cr	140	170	139	104	177	101	118	124	194	94.8	163	94.1	100	158
Co	22.7	30.7	21.0	20.1	18.7	19.7	23.2	16.5	20.8	29.0	24.4	22.0	17.6	25.5
Ni	70	95	58	49	73	86	56	41	79.0	72	72	173	39	69
Cu	32	29	7		32	33	27	<2	52.0	25	36	48	8	<2
Zn	82	141	118	85	83	91	90	44	84	93	84	69	77	67
As	3.1	3.6	3.6	3.2	8.33	12.4	2.4	3.76	3.98	3.24	2.88	4.22	4.86	4.09
Se	<1.4	<1.8	<1.5	<1.2	<1.8	2.2	<1.5	0.2	<1.9	2.0	<1.9	1.6	<1.8	<1.8
Rb	41.4	125.6	91.1	72.1	62.5	70.1	34.5	57.1	64.3	60.0	55.9	46.2	65.4	53.8
Sr	277	300	253	308	195	245	252	271	222	295	304	283	773	295
Y	9	29	19		19	15	12	10	20	19	16	20	12	21
Zr	131	156	132	168	142	169	136	148	163	173	165	145	192	155
Nb	10	11	10		10	9	10	9	10	10	10	9	9	10
Sb	0.28	0.36	0.30	0.28	0.37	0.36	0.25	0.28	0.41	0.24	0.29	0.25	0.22	0.32
Cs	2.49	6.08	5.32	4.20	3.62	4.12	2.24	3.98	3.72	3.40	2.63	2.91	3.25	3.64
Ba	605	947	792	583	543	542	506	696	530	588	681	584	1158	657
La	26.3	62.7	25.5	31.2	22.3	20.7	28.1	28.8	28.3	29.1	41.5	31.6	28.7	32.9
Ce	41.2	81.5	42.9	50.9	42.2	42.3	59.3	56.4	45.6	81.0	75.5	48.4	50.3	46.5
Nd	19.7	52.9	22.6	29.0	16.8	19.3	24.6	23.9	20.2	22.1	33.0	24.3	23.2	24.6
Sm	3.34	9.57	4.19	4.69	4.10	4.35	4.06	4.17	3.67	4.12	6.43	4.23	4.21	4.22
Eu	1.05	2.39	1.21	1.18	1.24	1.05	1.09	1.25	1.09	1.18	1.70	1.35	1.35	1.35
Gd	2.43	6.96	3.09	3.42	4.34	3.55	3.40	4.00	3.11	3.08	4.95	3.42	3.72	4.13
Tb	0.39	1.08	0.55	0.53	0.66	0.59	0.47	0.59	0.48	0.51	0.76	0.49	0.53	0.57
Tm	0.16	0.46	0.30	0.21	0.31	0.29	0.23	0.28	0.24	0.26	0.33	0.26	0.25	0.21
Yb	1.03	2.80	1.87	1.37	2.22	2.23	1.24	1.75	1.59	1.60	2.13	1.65	1.48	1.50
Lu	0.17	0.45	0.30	0.21	0.30	0.30	0.20	0.25	0.22	0.21	0.30	0.21	0.24	0.21
Hf	3.12	4.04	3.46	3.57	3.20	3.27	3.66	3.23	4.12	2.93	3.42	2.90	3.41	3.38
Ta	0.42	0.43	0.45	0.34	0.40	0.53	0.39	0.38	0.46	0.46	0.48	0.40	0.42	0.45

Table 3. Major and trace element composition of suevites and melt/glass fragments from the Bosumtwi impact structure.

	Suevite								Melt/glass fragment					
	LB-30a	LB-30b	LB-31b	LB-31a-6[a]	LB-39a	LB-39c	LB-41	LB-43	LB-40	LB-44	LB-45	LB-46	LB-47	LB-48
Au (ppb)	1.3	<1.4	1.3	2.2	0.8	1.5	2.3	1.70	0.8	0.8	0.8	1.9	0.9	0.7
Th	3.46	4.33	3.68	3.62	3.37	3.44	3.80	3.43	4.05	3.52	3.68	3.36	3.43	3.65
U	1.09	1.41	0.78	1.21	1.26	1.42	1.39	0.82	1.05	1.07	1.29	0.70	0.73	0.87
CIA	70	73	71		73	72	75	63	73	70	67	65	52	65
K/U	10,204	18,240	26,788	12,955	12,717	10,120	6626	17,103	13,912	13,179	8880	19,634	30,045	16,919
Th/U	3.16	3.07	4.72	3.01	2.67	2.42	2.73	4.19	3.84	3.30	2.86	4.83	4.71	4.19
La/Th	7.61	14.5	6.91	8.62	6.63	6.02	7.41	8.40	7.00	8.26	11.3	9.39	8.39	9.01
Zr/Hf	42	38.6	38.1	47.2	44.4	51.6	37.2	45.8	39.6	59.0	48.3	55.9	56.3	45.8
Hf/Ta	7.35	9.46	7.75	10.6	7.97	6.20	9.26	8.39	8.86	6.33	7.20	7.23	8.03	7.48
La_N/Yb_N	17.3	15.1	9.18	15.4	6.81	6.27	15.4	11.1	12.0	12.3	13.2	12.9	13.2	14.8
Gd_N/Yb_N	1.91	2.01	1.34	2.02	1.59	1.29	2.23	1.85	1.59	1.56	1.88	1.68	2.05	2.23
Eu/Eu^*	1.12	0.9	1.02	0.90	0.90	0.82	0.9	0.93	0.99	1.01	0.92	1.08	1.04	0.99

[a]Sample not analyzed by XRF (lack of material).
Major elements in wt%, trace elements in ppm, except as noted; all Fe as Fe_2O_3; blank spaces = not determined; N = chondrite-normalized (Taylor and McLennan 1985); chemical index of alteration (CIA) = $(Al_2O_3/[Al_2O_3 + CaO + Na_2O + K_2O]) \times 100$ in molecular proportions; $Eu/Eu^* = Eu_N/(Sm_N \times Gd_N)^{0.5}$.

are characterized by the presence of cross-cutting quartz veinlets. Much of the metasediment occurring at Bosumtwi has been sheared, and especially the graphitic shales often contain quartz ribbons (Figs. 2b and 2c). For example, sample LB-3a is composed of quartz bands intercalated with thin biotite-rich bands (Fig. 3a).

Meta-graywackes

The meta-graywackes are more massive and harder than the shales. They are medium-grained, light to dark gray, clastic rocks. Some samples have a weak foliation, and some are strongly mylonitized. Pyrite grains occur dispersed in some samples.

In thin section, these rocks are mainly composed of quartz, K-feldspar, plagioclase, mica, chlorite, and carbonate (Figs. 3b and 3c). The abundance of feldspar and poor sorting in the samples suggests the original sediments had not been transported too far from their source and therefore could represent turbidites. The plagioclase in some samples has been partially to completely altered to sericite; it may occur as relatively large porphyroclasts in some samples. Biotite is partially to completely altered to chlorite (Fig. 4). No evidence of shock deformation was found in any of the samples from this suite.

Granites

There are two types of granite samples in our suite: a fine- to medium-grained type (e.g., LB-10 and LB-18), which has been referred to as microgranite by some authors (e.g., Woodfield 1966), and a medium- to coarse-grained leucogranite (Fig. 5a). In thin section, the samples consist of quartz, feldspar (plagioclase and alkali feldspar), biotite, and muscovite, as well as some secondary sericite and chlorite. Most of the granites are altered, with most feldspar altered to sericite (Fig. 5b) and biotite to chlorite (Fig. 5c). Some other granite samples display seemingly oxidized biotite (e.g., sample LB-24; Fig. 6). Several granite samples (e.g., LB-19A and LB-25) display abundant graphic intergrowth of quartz and K- or alkali feldspar (Fig. 5c) and some spherulitic growths of feldspar. No evidence of shock deformation was found.

Suevites

The suevites are composed of melt clasts (including some partially devitrified glass) and clasts of the aforementioned country rock types in an optically unresolvable groundmass of target rock fragments, quartz, and phyllosilicates (including chlorite and sericite) (Figs. 7a and 7b). Whether or not the fine-grained groundmass contains small melt fragments is the subject of ongoing research. The clast population of suevites from the southern crater rim is comparatively more polymict, with both the banded and graphitic shales forming dominant clast types. This has imparted relatively darker gray color to the suevites from the south. Clast populations of suevites from

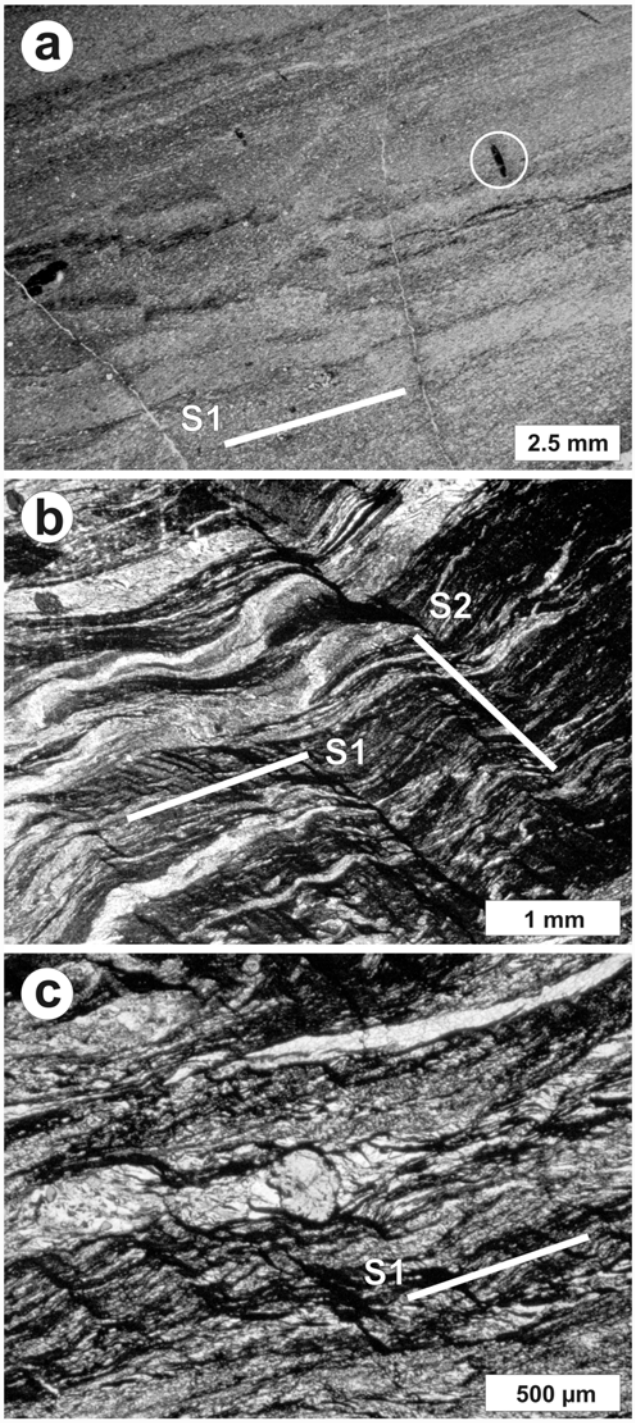

Fig. 2. a) Very fine-grained shale with some narrow, somewhat darker (carbon-rich?) layers and some relatively coarser-grained oxide grains (e.g., circle). Two thin, secondary veinlets of quartz cross-cut the S1 foliation (sample LB-5; plane-polarized light). b) A microphotograph (cross-polarized light) of well-banded graphitic shale with a mylonitic quartz ribbon (light colored); sample LB-51. c) A microphotograph of pervasive crenulation and microfolding; graphitic shale, sample LB-51.

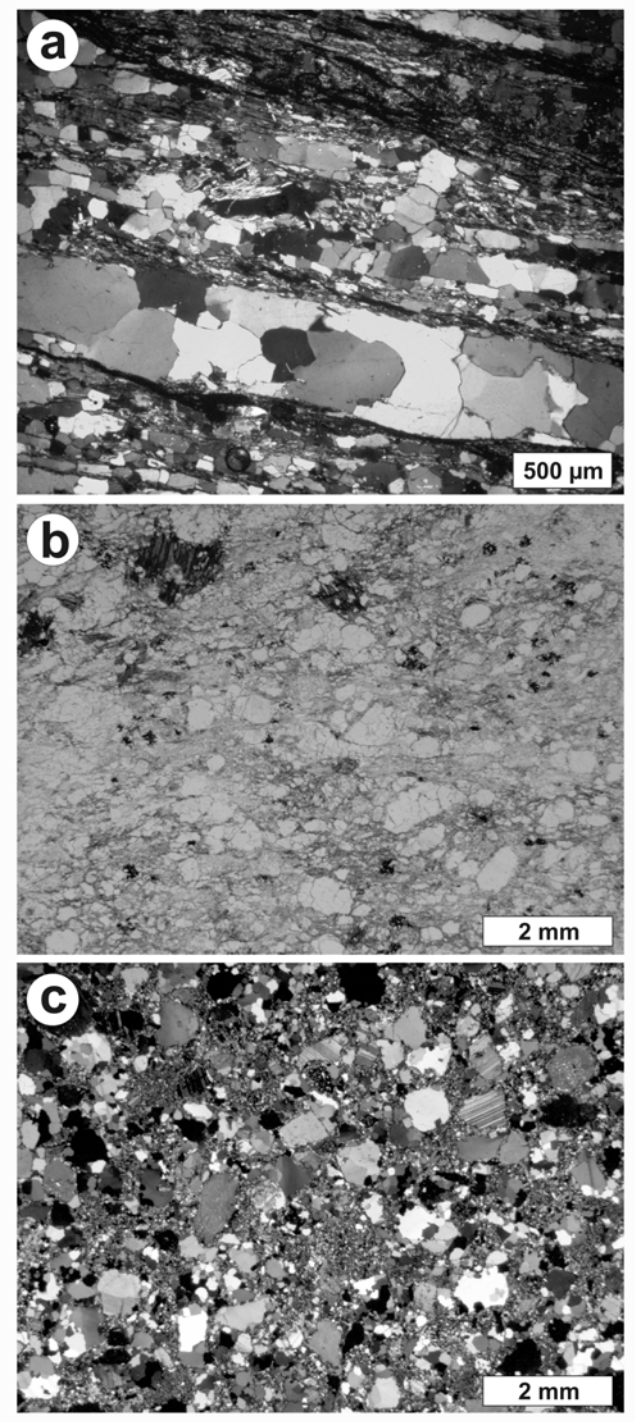

Fig. 3. a) Quartz-rich schist comprising quartz bands and relatively thinner biotite-rich bands; quartz is well sutured (sample LB-3a; cross-polarized light). b) Sheared, medium-grained meta-graywacke composed mainly of quartz and feldspar clasts, and minor biotite clasts (upper left) (sample LB-7; plane-polarized light). c) Barely deformed (note cross-cutting microfracture in central part of image), medium-grained meta-graywacke dominated by quartz (some recrystallized) and feldspar clasts in a fine-grained matrix of phyllosilicates, quartz, and feldspar (sample LB-33; cross-polarized light).

northern locations contain mostly meta-graywacke, and these samples are light gray in color.

The clasts in the suevites show different stages of shock metamorphism associated with the impact, as well as alteration of melt particles and some rock fragments. In thin section, some suevites show fresh glass clasts (highly vesicular or with flow structures) (Fig. 8a). Planar deformation features in quartz grains occur in one or two sets per grain (Fig. 8b). Crystals of quartz and feldspar, and even larger lithic clasts such as shale or schist, also show different stages of isotropization: the majority of the quartz grains in lithic clasts within suevite occur as diaplectic glass, and some have ballen texture. The suevites are characterized by alteration of the melt/glass clasts in the groundmass to phyllosilicates that so far have not been identified. Figures 7a and 7b show the argillic alteration of the groundmass of suevites to phyllosilicate minerals. This alteration of suevite components represents post-impact alteration, and the detailed study of these alteration effects in suevite, using X-ray diffraction (XRD) and infrared spectroscopy, will be discussed in a separate paper.

Melt/Glass Fragments

Melt and glass fragments from suevites are highly vesicular and very clast-poor. They usually consist of melt matrix and melted or vitrified clasts, with few (<5 vol%) crystalline clasts of quartz, meta-graywacke, phyllite, shale, granite, and quartzite. Some melt fragments show flow structures, and others are partially recrystallized. Diaplectic quartz and ballen quartz (Fig. 8c) are common in these melt/glass fragments.

Geochemistry

The results of major- and trace-element analyses, as well as some characteristic geochemical ratios, of the 36 analyzed samples are given in Tables 2 and 3. The average compositions of the various rock types are given in Table 4, together with the average composition of Ivory Coast tektites (with data from Koeberl et al. 1997, 1998; Boamah and Koeberl 2003) and upper continental crust rocks (Taylor and McLennan 1985).

Major Elements

The main country rocks (shale/phyllite, meta-graywacke, and granite) and the suevites and melt/glass fragments generally show some variation in their major element composition between the groups. There is also wide variation in the major element composition within the groups of the main country rocks, as well as some variation in the suevites and melt/glass fragments (Tables 2 and 3). In the Harker variation diagrams of Fig. 9, the quartz schist has the highest SiO_2 content with a value of 87.8 wt%. The SiO_2 contents of the granites, with an average value of 66.8 wt% and a range from 61.3 to 74.3 wt%, are higher than the contents of both the shales and the suevites. The suevites have an average SiO_2 content of 62.1 wt% and a range from 53.1 to 72.9 wt%, which is slightly lower than the SiO_2 content of the shale samples. The shale-phyllite average SiO_2 content is 64.0 wt%, with a range from 58.1 to 71.3 wt%. The melt fragments have an average SiO_2 content of 65.0 wt%, which is slightly higher than the SiO_2 content of the bulk suevites, and also have a more limited variation of SiO_2 content (from 61.3 to 68.1 wt%) than the bulk suevites. The CaO contents of the granites are slightly higher than those of the metasediment samples (shale/phyllite, arkose, and schist), with an average value of 1.10 wt% (±0.97 wt%) and a range from 0.12 to 3.14 wt%. The shales have an average CaO content of 0.50 wt%, with a range from <0.01 to 0.99 wt%. The suevites have an average CaO content of 0.82 wt%, with a range from 0.26 to 1.17 wt%, whereas the melt fragments have a much higher average CaO content of 1.53 wt%, with a range from 0.98 to 3.15 wt%. The loss on ignition (LoI) values of suevites are higher than the LoI values of the melt fragments, with an average value of 6.44 wt% (±1.90 wt%) and a range from 3.43 to 8.75 wt%, compared to the melt fragment average LoI of 4.54 wt% (±2.59 wt%), with a range from 0.53 to 7.40 wt%. Among the country rocks, the granite samples have lower LoI values than the metasediment samples; the shale samples have the highest LoI contents, with an average LoI value of 6.45 wt% (±3.11 wt%) and a range from 4.08 to 12.4 wt%. The granites have an average LoI of 3.47 wt% (±2.18 wt%), with a range from 0.53 to 7.36 wt%. The Fe_2O_3 (total Fe as Fe_2O_3) contents of suevite samples are slightly higher than those of the country rocks (meta-graywacke and granites), with an average content in suevite of 6.71 wt% (±1.64 wt%) and a range from 4.91 to 9.97 wt%, compared to the granites that have an average Fe_2O_3 content of 4.36 wt% (±2.26 wt%) and a range from 0.98 to 7.76 wt%. The shale-phyllite samples, however, have the highest Fe_2O_3 contents among the

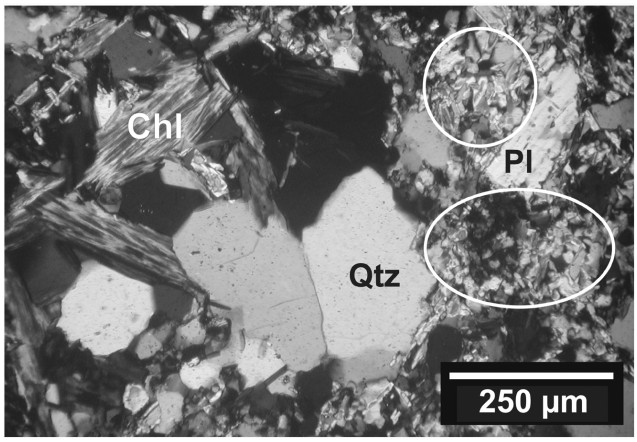

Fig. 4. Extensive alteration of biotite to chlorite (Chl) and of feldspar (mainly plagioclase = Pl) to sericite (see circle and ellipse) in meta-graywacke (sample LB-8; cross-polarized light).

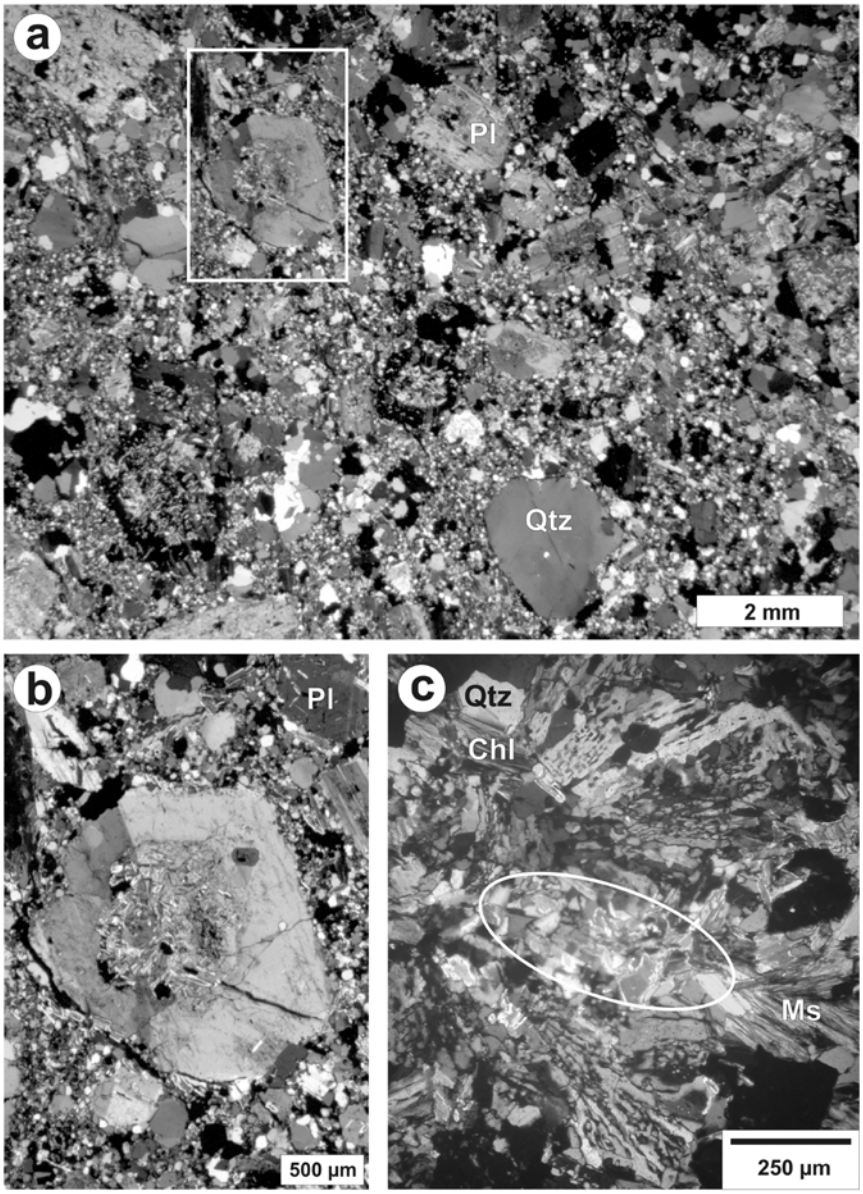

Fig. 5. Hydrothermally altered granite samples. a) Medium-grained granite with large feldspar (mostly plagioclase = Pl) and quartz (Qtz) (sample LB-26; cross-polarized light). b) Enlarged region (rectangle in [a]) containing a large euhedral crystal of alkali feldspar with a core. altered to sericite; a second plagioclase grain (Pl) is also indicated. c) Strong alteration in a fine-grained leucogranite indicated by chlorite (Chl) after biotite, and sericite (ellipse) in the interstices between larger granophyric intergrowths of quartz and albite, and muscovite (Ms) (sample LB-25; cross-polarized light).

analyzed samples, with an average content of 7.22 wt% and a range from 5.52 to 10.5 wt%. The melt fragments from the suevites have much higher Fe_2O_3 contents than the bulk suevites, with an average content of 6.01 wt% (±0.71 wt%), and a more limited variation in the Fe_2O_3 contents (from 4.62 to 6.59 wt%) than the bulk suevites.

The bulk suevites have low SiO_2/Al_2O_3 ratios, with an average value of 3.83 and a range from 2.51 to 5.94, and also relatively low K_2O/Na_2O ratios, with an average value of 0.97 and a range from 0.58 to 1.91. The melt fragments have slightly higher average SiO_2/Al_2O_3 and lower K_2O/Na_2O ratios than the bulk suevite. The country rocks have variable SiO_2/Al_2O_3 ratios, with the shale-phyllite samples having average SiO_2/Al_2O ratio of 4.41 (±1.47) and the granites having an average SiO_2/Al_2O ratio of 4.24 (±0.39). The shale-phyllite samples also have an average K_2O/Na_2O ratio of 2.69 (±2.58), which is higher than the average suevite K_2O/Na_2O ratio of 0.97 (±0.44). The degree of alteration in the country rocks and suevites may be inferred using chemical index of alteration (CIA) values (Rollinson 1993). The shale-pyllites, granites, melt fragments, and bulk suevites have average CIA values of 76 (range from 67 to 91), 62 (range from 48 to 78),

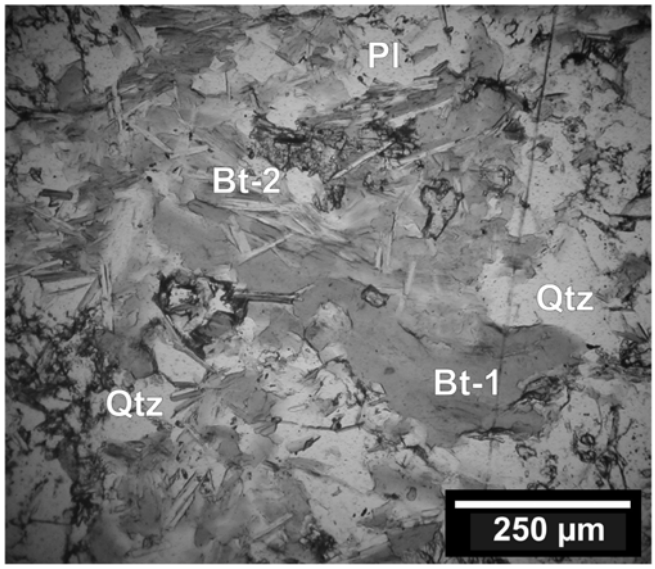

Fig. 6. Granite sample LB-24 (plane-polarized light), showing a partially oxidized biotite blast, Bt-1, and a smaller lath of unoxidized biotite, Bt-2. This sample is composed mainly of feldspar (mostly plagioclase = Pl), quartz (Qtz), biotite, and muscovite.

65 (range from 52 to 73), and 71 (range from 63 to 75), respectively.

Trace Elements

The country rocks and suevites show limited variation in trace element contents between the groups, but have some variability within groups. The siderophile and chalcophile elements, namely, Cr, Co, Ni, Cu, and V, are enriched in both country rocks and suevites by a factor of about 2 relative to their abundances in average upper crust (Taylor and McLennan 1985). The average Ni content in suevites (66 ppm) and average Ni content in shales (92 ppm) are about four times higher than the Ni abundance (20 ppm) in average upper continental crust (Taylor and McLennan 1985). Nickel contents in melt/glass fragments from suevites are somewhat higher than in bulk suevites (84 versus 66 ppm); Co contents are also slightly higher in the melt fragments (23.2 versus 21.6 ppm), but Cr contents are very similar (134 (±43) versus 134 (±28) ppm). The Ni values of bulk suevites and melt fragments are similar to the Ni contents reported for Birimian volcanic rocks by Sylvester and Attoh (1992) and those reported for some sulfide-mineralized samples from the Ashanti and Tarkwa mines by Dai et al. (2005). In the suevites, the contents of the high field strength elements (HFSE) Zr, Hf, Ta, Nb, U, and Th are not significantly different from values for the shallow-drilled suevites reported by Boamah and Koeberl (2003), except that Zr contents obtained in this study are slightly higher than those of the suevites from the shallow drilling outside the northern crater rim. The HFSE contents of the country rocks, especially the shales, are essentially similar to the values for Birimian graywackes and metapelites reported by Dai et al. (2005).

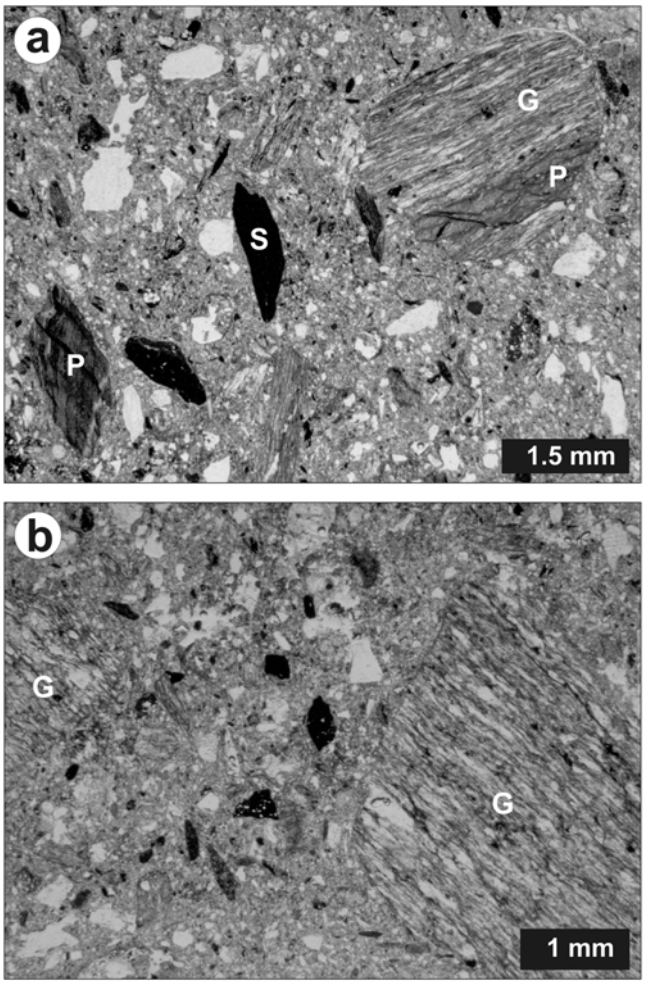

Fig. 7. a) Suevite with a variety of lithic clasts: mostly shale (S), phyllite (P) with crenulation, mylonitic fine-grained meta-graywacke (G), in an optically unresolvable phyllosilicate-rich groundmass (sample LB-39c; plane-polarized light). b) Mylonitic, fine-grained meta-graywacke clasts (G) in groundmass of mostly phyllosilicates (formed by the argillic alteration of melt clasts and smaller rock fragments), quartz grains, and opaque minerals (sample LB-39a; plane-polarized light).

Trace-element ratios also show some variability between the suevites and the country rocks, as well as variability within groups. The K/U, Th/U, La/Th, Zr/Hf, and Hf/Ta ratios of the suevites show limited variability compared to the variability within the country rocks. The Th/U, Zr/Hf, and Hf/Ta values for suevites have the following ranges: 2.42–4.72, 37.2–51.6, and 6.20–10.6 ppm, respectively, whereas the Th/U, Zr/Hf, and Hf/Ta values of shale-phyllites are 0.39–2.67, 34.8–72.3, and 5.62–28.4, respectively.

Rare Earth Elements (REE)

The C1 chondrite-normalized REE distribution patterns of the suevites and the various country rocks are shown in Fig. 10. They generally show patterns typical of Archean crustal rocks (Taylor and McLennan 1985), with light REE

(LREE) enrichment, lack of Eu anomaly or slightly negative/slightly positive Eu anomalies, and depleted heavy REE (HREE). Compared to the country rocks, the suevites show a very limited variation in their REE enrichment, with their chondrite-normalized patterns showing LREE enrichments (La_N/Yb_N ratios ranging from 6.27 to 17.3) and depletion in HREE (Gd_N/Yb_N ratio ranging from 1.29 to 2.23). The suevite patterns do not show significant Eu anomalies, with Eu/Eu* values ranging from 0.82 to 1.12 (average 0.94). The shale-phyllite samples have a rather wide variation in their REE abundance, and the patterns are characterized by LREE enrichment (La_N/Yb_N ratio ranging from 1.07 to 14.9), depletion in HREE (Gd_N/Yb_N ratio ranging from 0.51 to 3.14), and slightly negative Eu anomalies (Eu/Eu* values ranging from 0.80 to 0.95, with an average of 0.85). There is also no significant difference in the chondrite-normalized REE distribution pattern between the studied groups of samples and the average Ivory Coast tektites.

Provenance of the Main Country Rocks

In order to understand the effect of the high-energy Bosumtwi impact cratering event on the country rocks, it is important to understand not only the fundamental petrology and geochemistry of the country rocks, but also their provenance or tectonic setting. Here, we present the provenance studies of the country rocks, focusing mainly on the granites and meta-graywacke.

Granite Classification and Provenance

According to Leube et al. (1990), Na_2O, K_2O, CaO, and Rb are significant parameters in separating granitoids belonging to the Belt (Dixcove) type from those of the Basin (Cape Coast and Winneba) type, with the Belt-type having higher Na_2O and CaO contents, and lower K_2O and Rb contents than the Basin-type. The analyzed granite samples have average Na_2O and CaO contents of 3.87 (±1.17) wt% and 1.10 (±0.97) wt%, respectively, and average K_2O and Rb contents of 1.50 (±0.62) wt% and 48.7 (±17.6) ppm, respectively. In comparison with the average Na_2O, CaO, K_2O, and Rb contents of Basin granitoids (Winneba type) reported by Leube et al. (1990)—3.77, 2.30, 3.89 wt% and 152 ppm, respectively, and the average Na_2O, CaO, K_2O, and Rb contents of Belt granitoids (Dixcove type)—4.53, 3.24, 2.13 wt% and 53.4 ppm, respectively—most of the analyzed granite samples have high Na_2O contents. For example, the Na_2O content of LB-24 is 4.58 wt%, for LB-34 is 5.21 wt%, for LB-38 is 4.67 wt%, and for LB-50 the Na_2O content is 4.86 wt%. The CaO contents of these samples (e.g., LB-38 [0.16 wt%], and LB-50 [3.14 wt%]), however, are lower than the reported average Belt granitoid CaO content of 3.24 wt%. The analyzed granite samples have low K_2O and Rb contents in comparison to the average K_2O and Rb contents reported for the Belt granitoids (Leube et al. 1990) of 3.89 wt% and

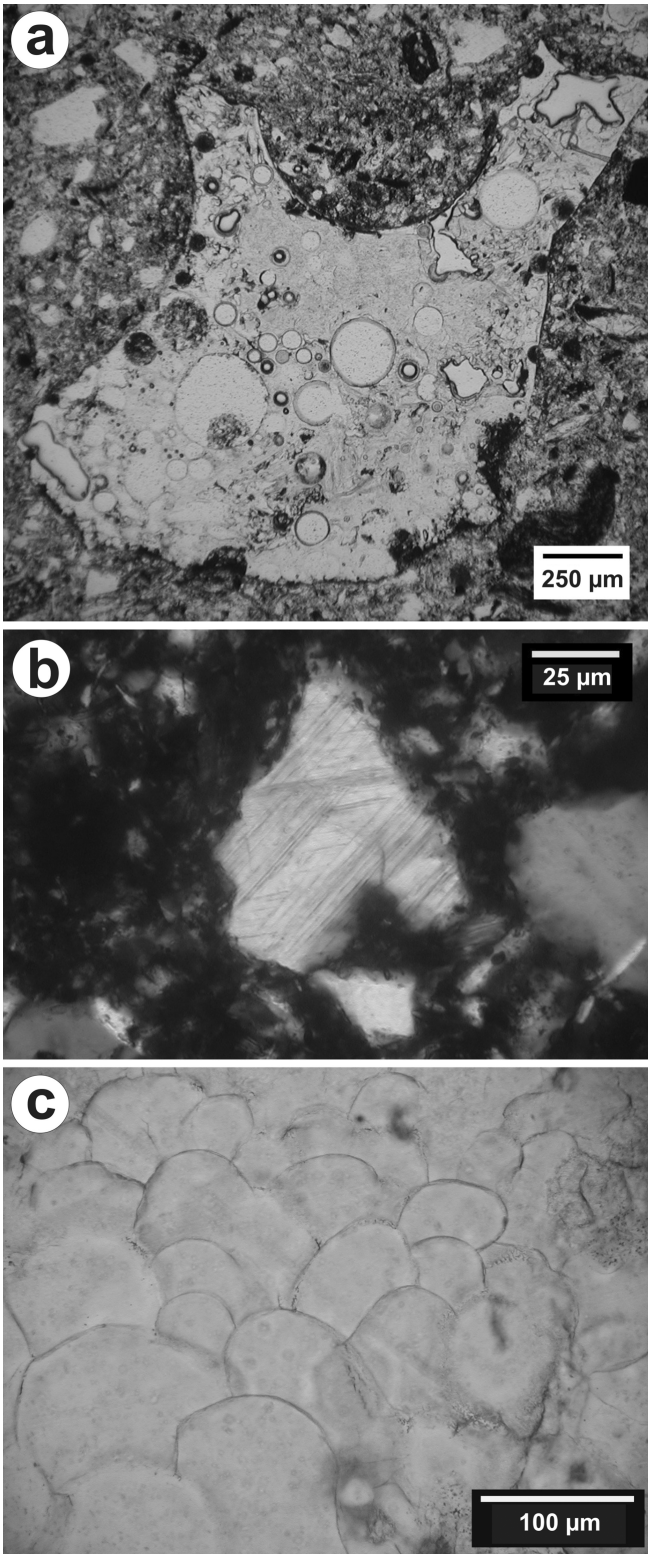

Fig. 8. a) A vesicular glass fragment in suevite; groundmass minerals include phyllosilicates and quartz (sample LB-43, plane-polarized light). b) Planar deformation features (2 sets) in quartz (clast in suevite, sample LB-43; cross-polarized light). c) Ballen quartz in suevite (sample LB-40; plane-polarized light).

Table 4. Average compositions (plus 1σ standard deviations) of analyzed country rocks, suevites, and melt fragments compared to average composition of Ivory Coast tektites and upper continental crust.

	Shale-phyllite (n = 6)		Granite (n = 9)		Suevite (n = 8)		Melt/glass fragments (n = 6)		Ivory Coast tektite average[a]	Upper contin. crust[b]
	Average	Range	Average	Range	Average	Range	Average	Range		
SiO_2	64.0 ± 4.88	58.1–71.3	66.8 ± 4.14	61.3–74.3	62.1 ± 5.92	53.1–72.9	65.0 ± 2.6	61.3–68.1	67.6	66.0
TiO_2	0.62 ± 0.25	0.13–0.81	0.58 ± 0.23	0.13–0.99	0.70 ± 0.11	0.50–0.82	0.65 ± 0.07	0.56–0.75	0.56	0.50
Al_2O_3	15.3 ± 3.01	9.70–18.0	15.8 ± 1.22	14.4–17.6	16.9 ± 2.86	12.3–21.1	16.4 ± 0.6	15.6–17.3	16.7	15.2
Fe_2O_3	7.22 ± 1.73	5.52–10.5	4.36 ± 2.26	0.98–7.76	6.71 ± 1.64	4.91–9.97	6.01 ± 0.71	4.62–6.59	6.16	4.50
MnO	0.06 ± 0.04	0.03–0.13	0.06 ± 0.03	0.01–0.11	0.07 ± 0.03	0.04–0.13	0.04 ± 0.01	0.03–0.07	0.06	
MgO	2.01 ± 0.90	0.44–3.20	2.60 ± 2.13	0.30–5.88	1.83 ± 0.73	0.79–2.61	1.13 ± 0.33	0.77–1.67	3.46	2.20
CaO	0.50 ± 0.35	<0.01–0.99	1.10 ± 0.97	0.12–3.14	0.82 ± 0.32	0.26–1.17	1.53 ± 0.81	0.98–3.15	1.38	4.20
Na_2O	1.30 ± 0.84	0.21–2.20	3.87 ± 1.17	1.57–5.21	2.07 ± 0.42	1.62–2.91	2.52 ± 0.72	1.69–3.78	1.90	3.90
K_2O	2.20 ± 0.84	0.56–2.75	1.50 ± 0.62	0.82–2.57	1.91 ± 0.64	1.11–3.10	1.82 ± 0.43	1.38–2.63	1.95	3.40
P_2O_5	0.16 ± 0.15	0.05–0.47	0.14 ± 0.08	0.02–0.24	0.09 ± 0.03	0.06–0.15	0.09 ± 0.06	0.05–0.22		
L.O.I	6.45 ± 3.11	4.08–12.4	3.47 ± 2.18	0.53–7.36	6.44 ± 1.90	3.43–8.75	4.54 ± 2.59	0.53–7.40	0.002	
Total	99.8		100.3		99.6		99.7		99.8	
SiO_2/ Al_2O_3	4.41 ± 1.47	3.30–7.35	4.24 ± 0.39	3.57–4.99	3.83 ± 1.08	2.51–5.94	3.98 ± 0.28	3.71–4.37	4.04	4.34
K_2O/ Na_2O	2.69 ± 2.58	0.97–7.82	0.41 ± 017	0.18–0.76	0.97 ± 0.44	0.58–1.91	0.75 ± 0.17	0.58–1.04	1.03	0.87
Sc	18.6 ± 3.0	15.7–23.6	11.4 ± 6.17	3.58–20.7	17.4 ± 3.5	14.0–25.5	16.5 ± 1.1	15.0–17.8	14.7	11
V	121 ± 15	95–131	84 ± 40	14–139	122 ± 27	86–150	98 ± 25	48–118		60
Cr	106 ± 31	80–162	146 ± 227	7–550	134 ± 28	101–177	134 ± 43	94–194	244	35
Co	17.0 ± 9.4	4.3–31.2	12.4 ± 7.80	0.98–24.0	21.6 ± 4.3	16.5–30.7	23.2 ± 4.0	17.6–29.0	26.7	10
Ni	92 ± 83	23–256	44 ± 49	9–135	66 ± 18	41–95	84 ± 46	39–173	157	20
Cu	50 ± 37	18–114	14 ± 5	<2–19.0	27 ± 10	7–33	34 ± 18	<2–52		25
Zn	100 ± 34	66–153	63 ± 22	25.00–96.0	92 ± 28	44–141	79 ± 10	67–93	23.0	71
As	13.6 ± 25.6	1.06–65.8	3.82 ± 3.95	0.93–13.2	5.05 ± 3.48	2.38–12.4	3.88 ± 0.71	2.88–4.86	0.45	1.5
Se	2.7 ± 4.7	0.2–12	1.3 ± 0.6	0.4–2.3	1.2 ± 1.4	0.2–2.2	1.8 ± 0.3	1.6–2.0	0.23	50
Rb	72 ± 29	22–95	48.7 ± 17.6	19.4–79.6	69 ± 29	34–126	58 ± 7	46–65	66.0	112
Sr	181 ± 89	65–320	430 ± 320	157–1205	263 ± 35	195–308	362 ± 203	222–773	260	350
Y	29 ± 22	5–64	12 ± 2	10–18	16 ± 7	9–29	18 ± 3	12–21		22
Zr	132 ± 34	93–181	151 ± 58	78–247	148 ± 15	131–169	165 ± 16	145–192	134	190
Nb	9.5 ± 2.1	6.1–12	10 ± 4	7–20	10 ± 1	9–11	10 ± 1	9–10		25
Sb	1.02 ± 1.55	0.11–4.02	0.19 ± 0.11	0.02–0.36	0.31 ± 0.05	0.25–0.37	0.29 ± 0.07	0.22–0.41	0.23	0.2
Cs	2.52 ± 1.03	0.81–3.66	2.28 ± 1.04	0.77–4.42	4.01 ± 1.29	2.24–6.08	3.26 ± 0.42	2.63–3.72	3.67	3.7
Ba	679 ± 290	344–1170	516 ± 381	168–1420	652 ± 152	506–947	700 ± 231	530–1158	327	550
La	27.3 ± 41.5	2.03–110	23.4 ± 19.0	7.61–71.2	30.7 ± 13.4	20.7–62.7	32.0 ± 4.96	28.3–41.5	20.7	30
Ce	57.6 ± 83.3	4.04–223	45.7 ± 32.9	18.5–127	52.1 ± 13.8	41.2–81.5	57.9 ± 16.0	45.6–81.0	41.7	64
Nd	28.6 ± 43.5	2.15–116	23.0 ± 16.5	6.17–61.7	26.1 ± 11.4	16.8–52.9	24.6 ± 4.44	20.2–33.0	21.8	26.0
Sm	6.01 ± 8.88	0.52–23.7	4.15 ± 2.70	1.15–10.3	4.81 ± 1.96	3.34–9.57	4.48 ± 0.98	3.67–6.43	3.95	4.50
Eu	1.52 ± 2.07	0.17–5.63	1.19 ± 0.70	0.32–2.77	1.31 ± 0.44	1.05–2.39	1.34 ± 0.21	1.09–1.70	1.20	0.88

Table 4. *Continued.* Average compositions (plus 1σ standard deviations) of analyzed country rocks, suevites, and melt fragments compared to average composition of Ivory Coast tektites and upper continental crust.

	Shale-phyllite (n = 6)		Granite (n = 9)		Suevite (n = 8)		Melt/glass fragments (n = 6)		Ivory Coast tektite average[a]	Upper contin. crust[b]
	Average	Range	Average	Range	Average	Range	Average	Range		
Gd	5.29 ± 7.01	0.80–19.2	3.13 ± 1.36	1.50–6.13	3.90 ± 1.36	2.43–6.96	3.73 ± 0.71	3.08–4.95	3.34	3.80
Tb	0.82 ± 0.91	0.14–2.55	0.45 ± 0.14	0.25–0.68	0.61 ± 0.21	0.39–1.08	0.56 ± 0.10	0.48–0.76	0.56	0.64
Tm	0.37 ± 0.22	0.16–0.74	0.19 ± 0.05	0.11–0.27	0.28 ± 0.09	0.16–0.46	0.26 ± 0.04	0.21–0.33	0.30	0.33
Yb	2.51 ± 1.40	1.28–4.96	1.29 ± 0.47	0.65–2.11	1.81 ± 0.59	1.03–2.80	1.66 ± 0.24	1.48–2.13	1.79	2.20
Lu	0.38 ± 0.19	0.20–0.67	0.18 ± 0.08	0.06–0.33	0.27 ± 0.09	0.17–0.45	0.23 ± 0.03	0.21–0.30	0.24	0.32
Hf	2.96 ± 0.74	2.36–4.19	3.64 ± 1.66	2.28–6.72	3.44 ± 0.31	3.12–4.04	3.36 ± 0.44	2.90–4.12	3.38	5.80
Ta	0.41 ± 0.17	0.08–0.57	0.50 ± 0.40	0.20–1.30	0.42 ± 0.06	0.34–0.53	0.45 ± 0.03	0.40–0.48	0.34	2.20
Au (ppb)	4.5 ± 5.9	0.2–15	0.9 ± 0.6	0.0–1.9	1.6 ± 0.5	0.8–2.3	1.0 ± 0.5	0.7–1.9	0.56	1.80
Th	3.26 ± 0.83	2.44–4.64	3.61 ± 2.12	1.48–8.37	3.64 ± 0.32	3.37–4.33	3.62 ± 0.24	3.36–4.05	3.54	10.7
U	2.59 ± 1.88	1.12–6.20	1.23 ± 0.66	0.65–2.72	1.17 ± 0.26	0.78–1.42	0.95 ± 0.23	0.70–1.29	0.94	2.8
CIA	76	67–91	62	48–78	71	63–75	65	52–73	76	46
K/U	9855 ± 6407	1842–16,189	10,875 ± 3566	7619–18,785	14,344 ± 6288	6626–26,788	17,095 ± 7309	8880–30,045	17,287	10,076
Th/U	1.71 ± 0.84	0.39–2.67	3.02 ± 1.10	1.86–5.45	3.25 ± 0.80	2.42–4.72	3.95 ± 0.78	2.86–4.83	3.77	3.82
La/Th	10.0 ± 17.3	0.54–44.9	6.55 ± 2.38	1.74–10.3	8.26 ± 2.7	6.02–14.5	8.89 ± 1.42	7.00–11.3	5.85	2.8
Zr/Hf	45.9 ± 13.6	34.8–72.3	43.3 ± 9.73	25.7–55.8	43.1 ± 5.06	37.2–51.6	49.8 ± 7.04	39.6–59.0	39.6	32.8
Hf/Ta	10.1 ± 8.99	5.62–28.4	8.93 ± 3.07	4.30–12.0	8.38 ± 1.38	6.20–10.6	7.52 ± 0.86	6.33–8.86	9.94	2.64
La_N/Yb_N	5.07 ± 5.43	1.07–14.9	15.0 ± 15.7	3.50–53.4	12.1 ± 4.29	6.27–17.3	13.1 ± 0.97	12.0–14.8	7.81	9.21
Gd_N/Yb_N	1.28 ± 0.98	0.51–3.14	2.30 ± 1.57	0.97–5.52	1.78 ± 0.34	1.29–2.23	1.83 ± 0.27	1.56–2.23	1.51	1.4
Eu/Eu_*	0.85 ± 0.06	0.80–0.95	0.99 ± 0.13	0.70–1.19	0.94 ± 0.09	0.82–1.12	1.00 ± 0.05	0.92–1.08	1.01	0.65

[a]Data from Koeberl et al. (1998).

[b]Data from Taylor and McLennan (1985).

Major elements in wt%, trace elements in ppm, except as noted; all Fe as Fe_2O_3; n = number of samples; blank spaces = not determined; N = chondrite-normalized (Taylor and McLennan 1985); chemical index of alteration (CIA) = $(Al_2O_3/[Al_2O_3 + CaO + Na_2O + K_2O]) \times 100$ in molecular proportions; $Eu/Eu^* = Eu_N/(Sm_N \times Gd_N)^{0.5}$.

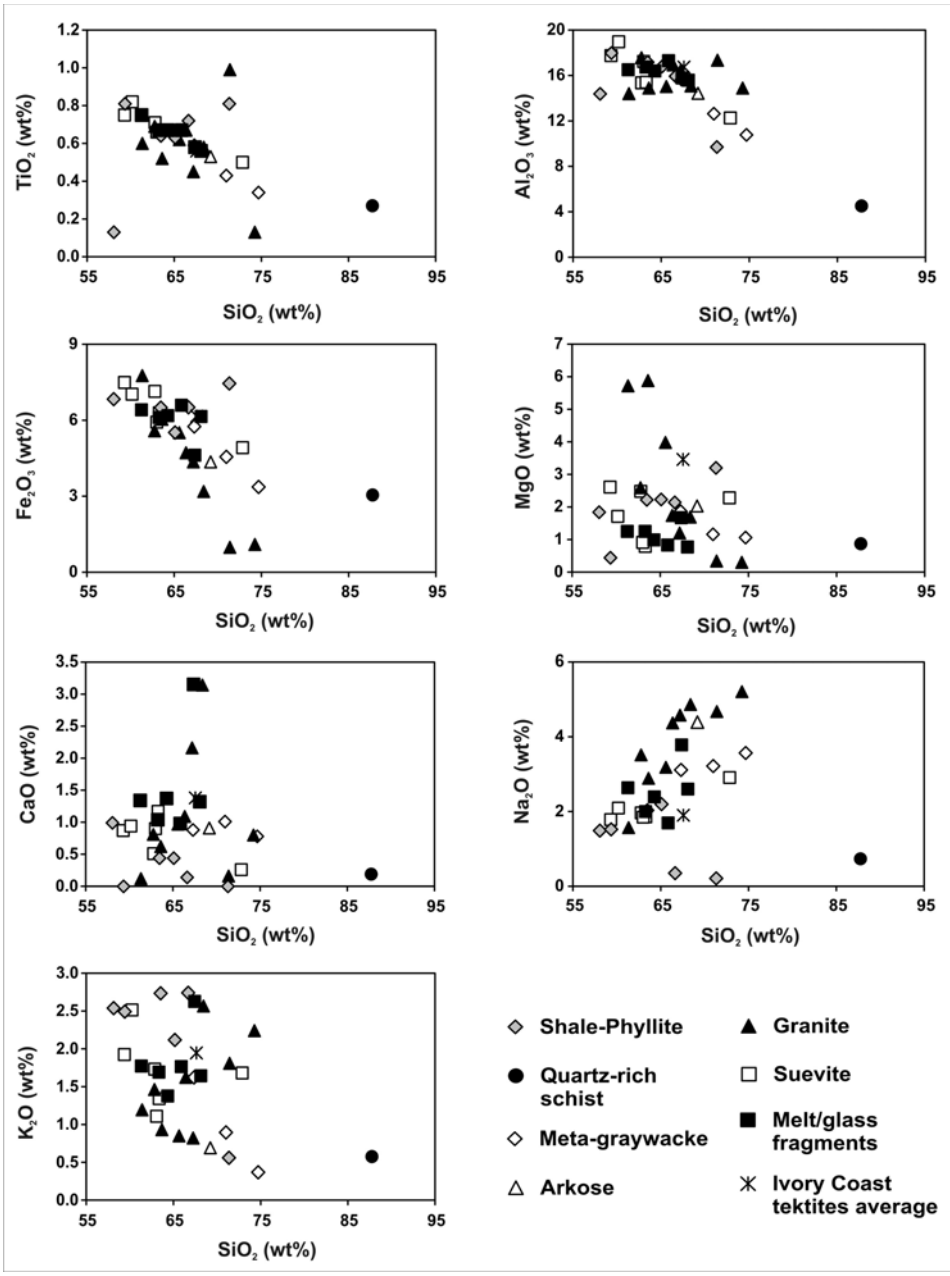

Fig. 9. Harker variation diagrams for metasedimentary lithologies, granite, suevite, and melt/glass fragments in suevites compared to the average values for Ivory Coast tektites (with data from Koeberl et al. 1997, 1998; Boamah and Koeberl 2003).

152 ppm, respectively. These values are also comparable to a Belt-type granite sample reported in John et al. (1999), with 3.59 wt% CaO, 4.58 wt% Na_2O, 1.89 wt% K_2O, and 50 ppm Rb. The published CaO content of this Belt-type sample is, thus, far higher than the CaO contents of the samples analyzed here.

The total alkali element abundance (Na_2O and K_2O)–silica diagram, TAS (Fig. 11), after Cox et al. (1979), shows that most of the Bosumtwi granites have a dioritic to quartz-dioritic composition. Pearce et al. (1984) classified granites into ocean-ridge granites (ORG), volcanic-arc granites (VAG), within-plate granites (WPG), and syn-collisional granites (syn-COLG) using discrimination diagrams based on the trace elements Nb, Y, Ta, and Yb. The Nb-Y discrimination diagram in Fig. 12a indicates that the Bosumtwi granites belong to a VAG or syn-COLG tectonic setting. However, this discrimination diagram is ambiguous, as VAG cannot be distinguished from syn-COLG. In contrast, the Ta-Yb diagram of Fig. 12b shows the fields of VAG and syn-COLG. It is clear that the Bosumtwi granites relate to a VAG setting and, therefore, might have a genetic association with the metavolcanic package in the Ashanti belt. This

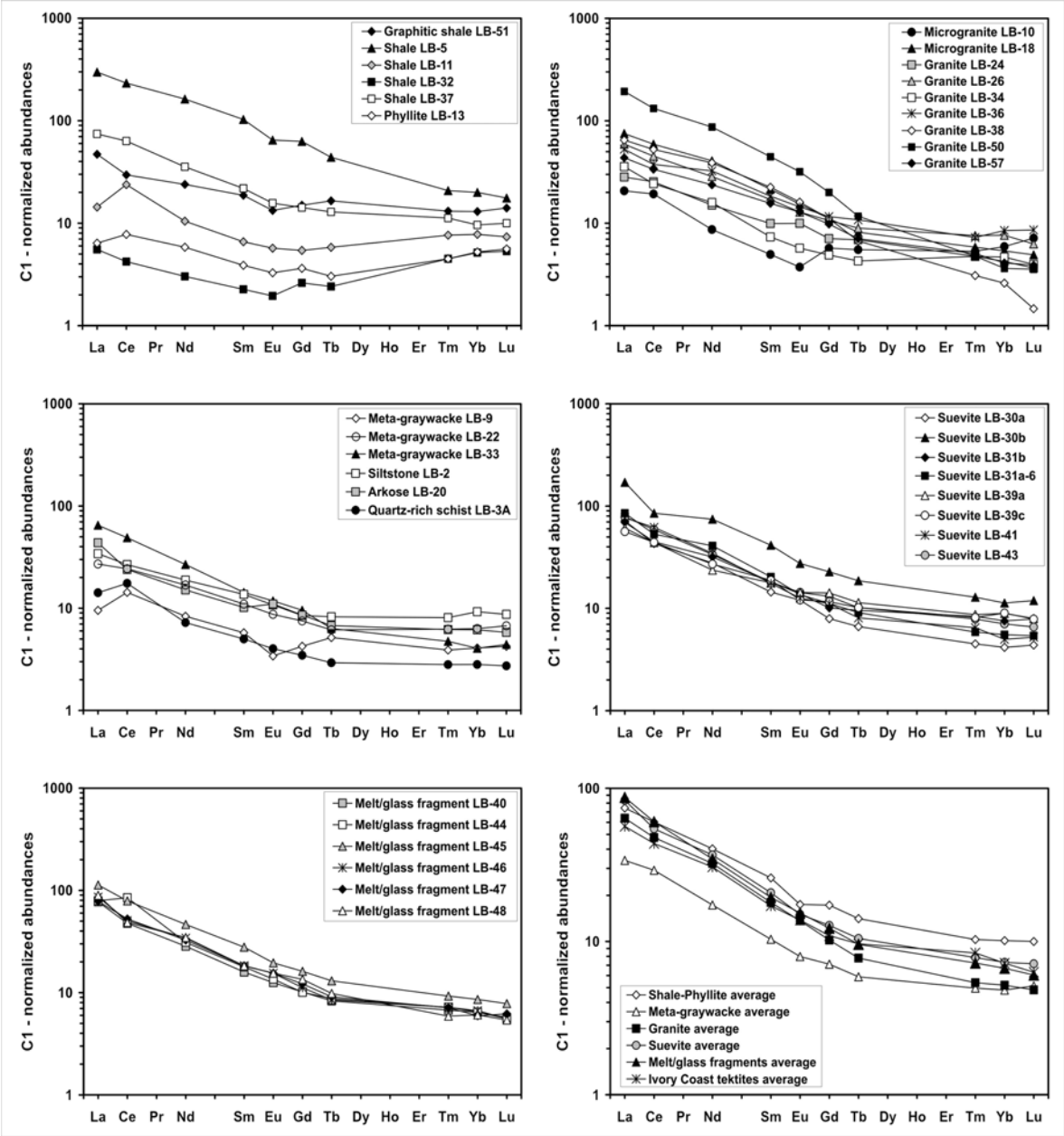

Fig. 10. Chondrite (C1)-normalized rare earth element (REE) patterns for the various sample groups (shale-phyllite, granite, meta-graywacke, and suevite), as well as averages for these groups and average of the Ivory Coast tektites (with data from Koeberl et al. 1997, 1998 and Boamah and Koeberl 2003). Normalization factors from Taylor and McLennan (1985).

conclusion is, however, preliminary, as a more representative sample suite needs to be studied.

Metasediment Classification and Provenance

The use of detrital modes of sandstone grains to study provenance was described by Dickinson and Suczek (1979). This method is based on the fact that sandstone compositions are directly influenced by the character of the sedimentary provenance and that the key relations between provenance and basin are governed by plate tectonics. The relative proportions of terrigenous sandstone grains are therefore guides to the nature of the source rocks in the provenance terrane from which sandy detritus was derived. The method has been used by many authors for sandstone provenance studies (e.g., Dickinson et al. 1983; Mader and Neubauer 2004; Osae et al. 2006) and focuses mainly on proportions of detrital framework grains.

For this study, thin-section point counting of four meta-graywacke samples was carried out to establish their quantitative modal composition. The modal analysis was done by counting more than 1000 points per thin section. The results are presented in Table 6. Mineral grains less than

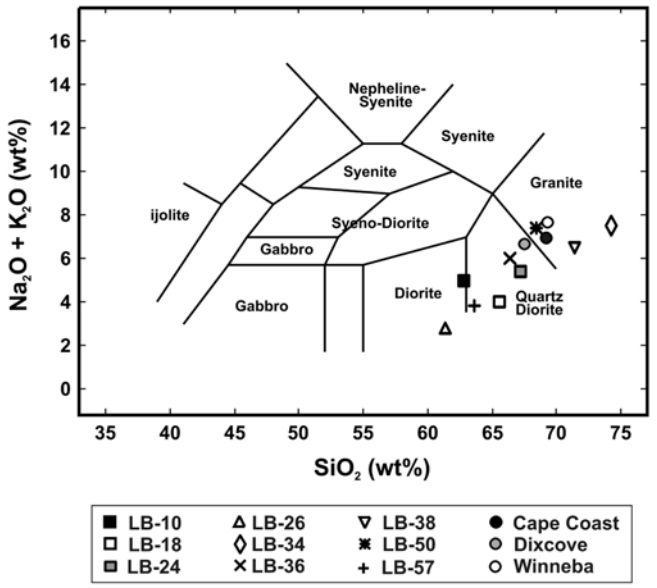

Fig. 11. Provenance classification of Bosumtwi granites, using a total alkali-silica (TAS) plot (after Cox et al. 1979). This indicates that the granites have tonalitic to dioritic composition. Granitoid averages data from Leube et al. (1990) are plotted for comparison (Cape Coast and Winneba types are sedimentary basin granitoids, the Dixcove type represents volcanic belt granitoids).

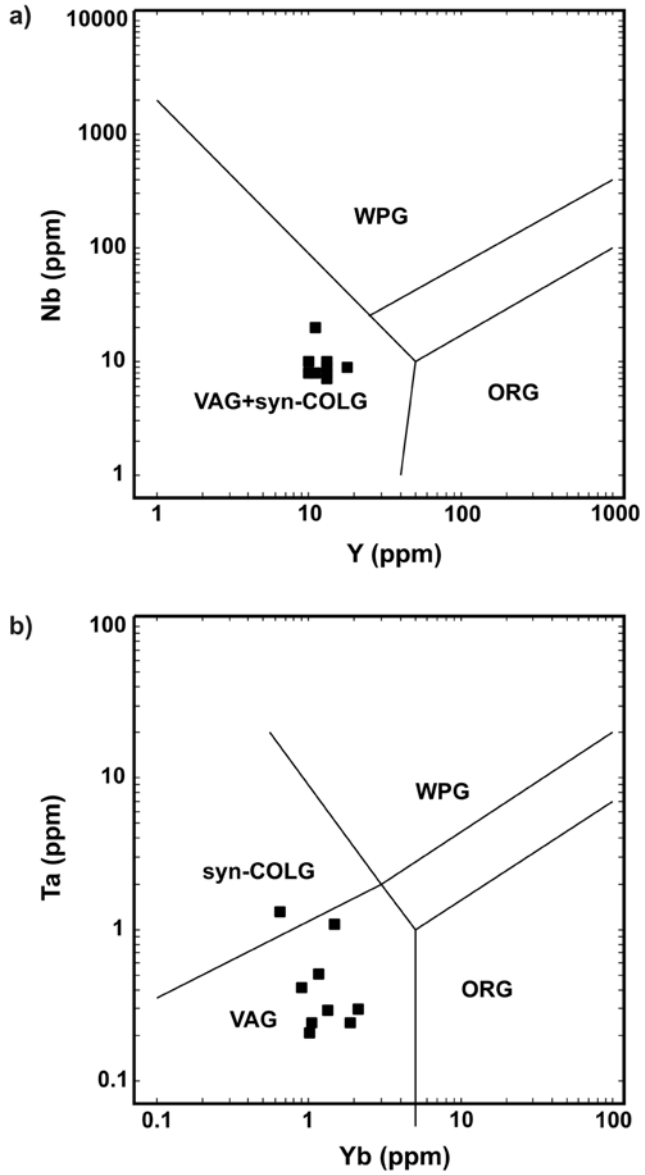

Fig. 12. a) Composition of Bosumtwi granites plotted in a Nb-Y discrimination diagram (after Pearce et al. 1984), showing the fields of volcanic-arc granites (VAG), syn-collisional granites (syn-COLG), within-plate granites (WPG), and ocean-ridge granites (ORG). The Bosumtwi granites fall into the VAG or syn-COLG fields. b) Ta-Yb discrimination diagram for the Bosumtwi granites, separating the fields for VAG and syn-COLG granites (Pearce et al. 1984). The Bosumtwi granites seem to relate mostly to a volcanic-arc granite (VAG) provenance.

0.064 mm apparent diameter were counted as matrix. The matrix of the meta-graywackes is generally composed of secondary minerals, such as sericite and chlorite. Modal compositions of the samples were recalculated as volumetric proportions of the framework categories described by the Gazzi-Dickinson method (e.g., Dickinson and Suczek 1979). The framework categories are monocrystalline quartz (Qm); polycrystalline quartz (quartzose grains) (Qp); feldspar (F), including plagioclase (P) and K-feldspar (K); lithic grains other than quartzose grains (L); and total lithic fragments (Lt), which comprises both L and Qp; the results of the recalculation in vol% are presented in Table 7.

According to Okada (1971), triangular diagrams of detrital modes could also be used in the classification of sandstones using quartz, feldspar, and lithic fragments. The Qm-F-Lt classification diagram in Fig. 13a shows the studied samples are of lithic meta-graywacke composition. The resulting Q-F-L and Qm-F-Lt ternary provenance diagrams (e.g., Dickinson et al. 1983; Mader and Neubauer 2004; Osae et al. 2006) are shown in Figs. 13b and 13c. The Qm-F-Lt ternary provenance plot (Fig. 13b) shows that the studied Birimian meta-graywackes fall between the magmatic arc field and the recycled orogen field, within the undissected arc, the transitional arc, and the lithic recycled subfields; on the other hand, the Q-F-L ternary provenance shows them to belong only to the recycled orogen field. Dickinson and Suczek (1979) described sediments from an undissected arc provenance to be largely of volcaniclastic debris shed from volcanogenic highlands along active island arcs and that sites for deposition include trenches and fore arc basins. Sediments of recycled orogen provenance, on the other hand, are described as recycled detritus derived from uplifted terranes of folded and faulted strata.

In order to resolve this ambiguity in the interpretation of the two detrital mode diagrams, we used geochemical discrimination diagrams to classify and characterize the tectonic setting of the metasediments. For this we used the

Table 5. Average Fe_2O_3, V, Cr, and Co contents of analyzed metasediments compared to average compositions of other Birimian metasediment samples (about 50 km southeast of Bosumtwi crater) published in Asiedu et al. (2004).

	This work				Asiedu et al. 2004			
	Shale-phyllite (*n* = 6)		Meta-graywacke (*n* = 3)		Meta-graywacke (*n* = 19)		Metapelites (*n* = 5)	
	Average	Range	Average	Range	Average	Range	Average	Range
Fe_2O_3	7.22 ± 1.73	5.52–10.5	4.56 ± 1.19	3.37–5.75	7.01 ± 1.00	5.50–8.56	10.6 ± 1.92	8.79–13.7
V	121 ± 14.8	95.2–131	94.2 ± 23.8	77.4–111	156 ± 40.8	102–226	169 ± 51.8	126–254
Cr	106 ± 31	80.0–162	57.0 ± 19.1	45.5–79.0	173 ± 106	54.0–529	165 ± 28.1	127–193
Co	17.0 ± 9.40	4.29–31.2	15.1 ± 5.65	10.7–21.4	64.6 ± 26.4	40.8–166	57.6 ± 13.7	48.4–81.9

Major elements in wt%, trace elements in ppm. Total Fe as Fe_2O_3. Blank spaces = not determined; *n* = number of samples analyzed.

Table 6. Results of point counting of thin sections of meta-graywackes (data in vol%).

		Meta-graywacke samples			
		LB-7	LB-8	LB-19B	LB-33
Quartz (Qm)		7.4	6.3	5.1	9.1
Feldspar (F)	K	7.0	4.7	7.5	11.0
	P	2.4	2.4	4.6	8.0
	Total	9.4	7.1	12.1	19.0
Lithic fragment (Lt)	Qp	28.4	25.6	23.9	30.3
	Q-F	9.7	8.1	10.2	4.6
	Q-B	3.0	5.8	4.6	–
	K-P	–	–	0.4	–
	F-B	0.1	–	0.4	–
	Q-F-B	0.05	0.4	2.1	–
	Chert	5.4	0.7	–	17.4
	Total	47.1	40.6	41.8	52.3
Biotite (B)		2.8	–	0.8	–
Chlorite (CH)		–	2.0	–	–
Matrix		30.0	41.0	37.6	11.4
Opaque		2.7	0.7	4.3	3.0
Accessory		0.75	2.0	0.2	–
Total counts		1057	1209	1408	1257

Grain parameters: Qm = monocrystalline quartz; Qp = polycrystalline quartz (quartzose grain); K = K-feldspar; P = plagioclase; F = K+P; Lt = total polycrystalline lithic fragments; Q-B = quartzose grain with biotite; Q-F-B = quartzose grain with both feldspar and biotite.

Table 7. Recalculated framework modes of the studied meta-graywacke samples (data in vol%).

					QFL			QmFLt		
	Qm	Qp	K	P	Q	F	L	Qm	F	Lt
LB-7	11.6	44.4	11.0	3.7	56.0	14.7	29.3	11.6	14.7	73.8
LB-8	11.6	47.5	8.73	4.44	59.1	13.2	27.7	11.6	13.2	75.2
LB-19B	8.72	40.5	12.7	7.74	49.3	20.4	30.3	8.72	20.4	70.9
LB-33	11.3	37.7	13.6	9.99	49.0	23.6	27.4	11.3	23.6	65.1

Grain parameters: Qm = monocrystalline quartz; Qp = polycrystalline quartz (quartzose grain); K = K-feldspar; P = plagioclase; L = lithic fragments except Qp; F = K+P; Lt = total polycrystalline lithic fragments.

geochemical data of all the metasedimentary rocks, i.e., 6 shale-phyllite, 3 meta-graywacke, 1 siltstone, and 1 arkose samples. The chemical classification diagrams of the metasedimentary rocks are shown in Figs. 14a and 14b. The high abundance of alteration minerals (e.g., sericites and chlorites) causes a few of the samples to plot in the arkose field. The La-Th-Sc ternary plot with fields defined by Girty and Barber (1993) is shown in Fig. 15a. It shows most of the metasedimentary samples belong to or are close to the magmatic arc-related field. Two out of the 3 meta-graywacke samples fall into the magmatic-arc field. According to Bhatia and Crook (1986), four fields of principal tectonic settings can be distinguished using the trace elements Th, Co, and Zr. These are the passive margin (PM; recycled sedimentary and metamorphic source rocks), active continental margin (ACM; granites, gneisses, siliceous volcanics), continental island arc (CIA; felsic volcanic source rocks), and oceanic island arc (OIA; calc-alkaline or tholeiitic rocks) fields. In Fig. 15b, the Birimian metasediment samples plot into or close to the fields for the OIA and CIA tectonic settings.

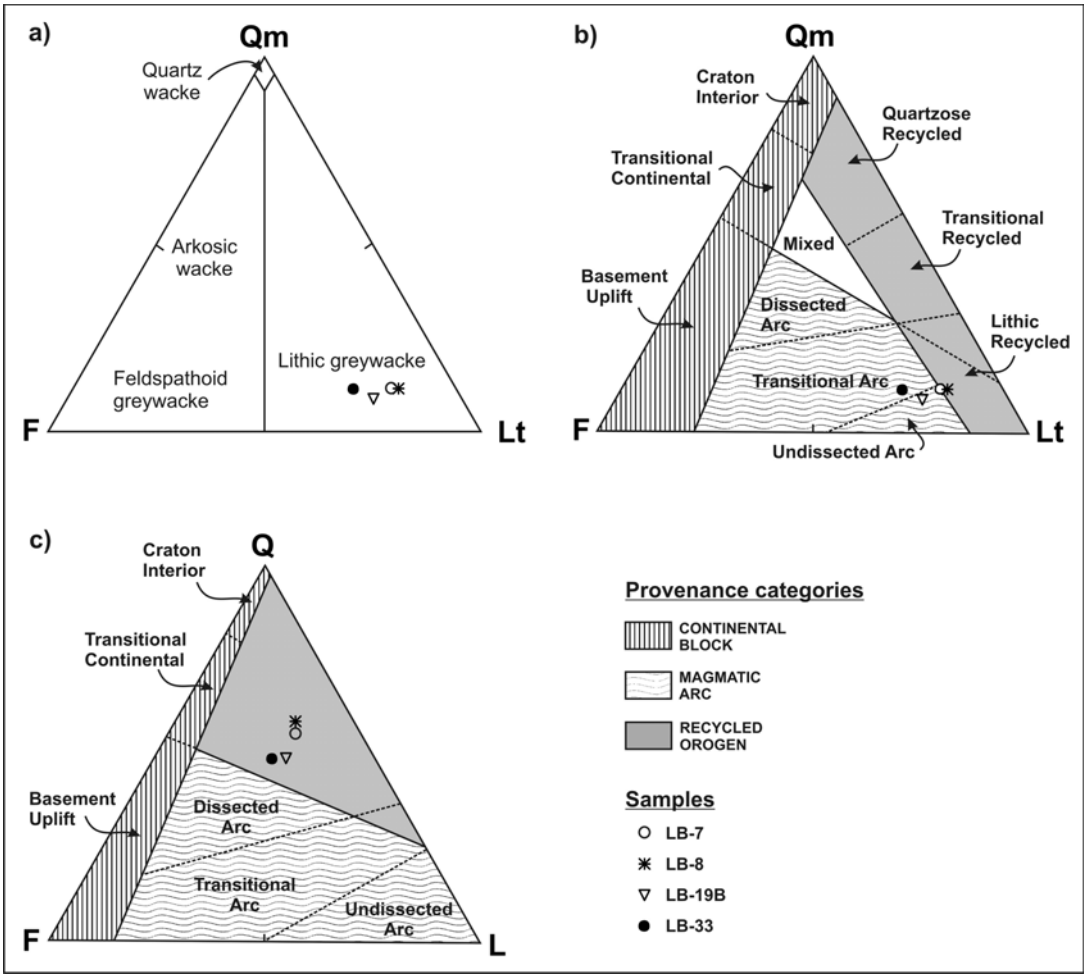

Fig. 13. a) Qm-F-Lt (monocrystalline quartz, feldspar, lithic fragments) classification diagram for meta-graywackes (after Okada 1971), showing the fields of the various types of wackes. Here, the Bosumtwi meta-graywacke samples belong to the field of the lithic graywacke. b) Qm-F-Lt diagram for provenance discrimination (after Dickinson et al. 1983) showing the various provenance fields and subfields. In this diagram the samples are classified into the undissected arc subfield of a magmatic arc. c) Q-F-L (both monocrystalline and polycrystalline quartz, feldspar, lithic fragments) provenance discrimination diagram (after Dickinson et al. 1983) for the Bosumtwi samples. The samples in this diagram fall into the field for the recycled orogen provenance.

The above classification and discrimination diagrams indicate, therefore, that the Bosumtwi metasediments relate to a magmatic arc setting. The volcaniclastic debris was perhaps derived from volcanogenic highlands along an active island arc or from a continental margin. This interpretation is supported by data presented in Leube et al. (1990), Taylor et al. (1992), Asiedu et al. (2004), and Feybesse et al. (2006). Leube et al. (1990) suggested the magmatism and sedimentation in the Birimian to be coeval. On the basis of geochronological studies (Rb-Sr, Pb/Pb, and Sm-Nd analyses) of the Birimian rock units, Taylor et al. (1992) concluded that the Birimian sediments were derived from the adjacent penecontemporaneous volcanic belts, with no detectable input from any significantly older terrane. On the basis of trace element data from the Birimian metasedimentary rocks, Asiedu et al. (2004) also suggested that the Birimian metasedimentary rocks were mainly derived from a juvenile arc source of mixed felsic and mafic composition. Feybesse et al. (2006), in their geodynamic model of the Paleoproterozoic Birimian province, also favored the emplacement of a juvenile basic volcanic-plutonic rocks accompanied by the deposition of the graywacke sediments.

DISCUSSION

Alteration in the Country Rocks

Alteration is the compositional change that occurs after the formation of a rock and may be due to metamorphically or magmatically triggered activity. In the context of impact structures, it may also be induced by hydrothermal activity triggered by impact (Koeberl and Reimold 2004). The Bosumtwi country rocks have undergone various alteration

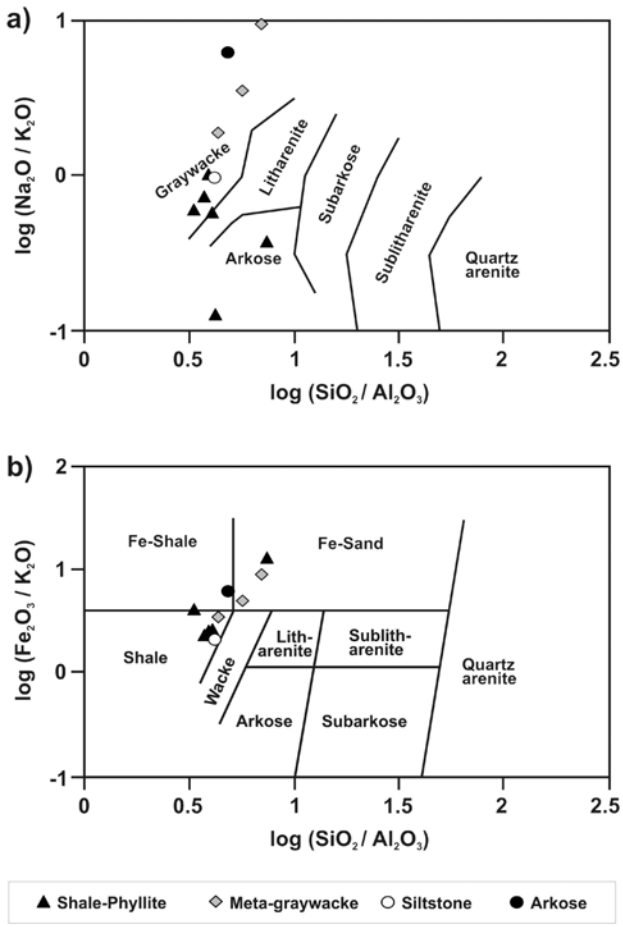

Fig. 14. a) Classification diagram (after Pettijohn et al. 1972) discriminating the metasedimentary rock samples by their logarithmic ratios of SiO_2/Al_2O_3 and Na_2O/K_2O. b) Classification diagram (after Herron 1988) discriminating metasedimentary rock samples by their logarithmic ratios of SiO_2/Al_2O_3 and Fe_2O_3/K_2O.

processes and were subject to various elevated temperature and pressure conditions associated with a number of metamorphic events. The Eburnean event (~1.9–2.1 Gyr ago), which is the last tectonothermal event to have stabilized the West African craton (Wright et al. 1985; Leube et al. 1990), caused the Birimian supracrustal sequences to become folded and metamorphosed to greenschist facies. Feybesse et al. (2006) considered the Eburnean event to have involved several phases: a D1 thrust tectonic phase (2.13 to 2.105 Gyr) involved crustal thickening through unit stacking and was related to horizontal crustal shortening; this was followed by D2–3 events, from 2.095 to 1.98 Gyr, which involved a period of strike-slip movement.

Pre-Impact Hydrothermal Alteration

The pre-impact hydrothermal activity and associated gold mineralization in the Birimian, according to the evolution model for the Birimian Supergroup by Eisenlohr and Hirdes (1992), is associated with late Eburnean-stage lateral strike slip and dextral shearing along the boundaries between the metavolcanic and metasedimentary Birimian units. The hydrothermal process resulted in the greenschist mineral assemblages of the Birimian rocks forming new minerals under different conditions of temperature, pressure, and fluid composition. Some minerals were also replaced by metasomatism (e.g., addition of H_2O and CO_2). According to Woodfield (1966), the widespread presence of hydrous minerals, such as chlorite, epidote, and sericite, the consistent presence of carbonates (ankerite and calcite), and the presence of these minerals in veins give evidence of involvement of carbon dioxide and water metasomatism. Carbonate thermometry is based on the use of actual carbonate solvi (Rosenberg 1967). On the basis of the mole% $FeCO_3$ content in siderite, Manu (1993) suggested 350 °C as the temperature of the hydrothermal alteration event that affected the Ashanti belt in which the Bosumtwi structure occurs. On the basis of fluid inclusion studies, Dzigbodi-Adjimah (1993) also suggested that the hydrothermal activity took place at about 350 °C and involved dilute aqueous solutions. According to Yao and Robb (2000), hydrothermal alteration minerals at the Obuasi mine (south of the crater, in the Ashanti belt) are dominated by quartz, sericite (muscovite), sulphides (mainly pyrite and arsenopyrite), and carbonates. From thermodynamic calculations, Yao and Robb (2000) derived that the initial homogeneous H_2O-CO_2-rich fluid contained 50–80 mole% H_2O at 300–350 °C and 2 kbar.

In this study we observed that some of the country rock samples (e.g., granites LB-18 and 34; meta-graywacke LB-7, 19B, and 33; and shale LB-11 and 32) display the mineral assemblage plagioclase-quartz-biotite-chlorite±epidote± muscovite, which is a typical metamorphic mineral assemblage for greenschist facies Birimian rocks (John et al. 1999). Other samples (e.g., granites LB-25, 26, and 38, meta-graywacke LB-8, and shale LB-5) display the mineral assemblage plagioclase-quartz-chlorite-sericite±sulfides± sphene. In these altered samples, most plagioclase is replaced by sericite, and biotite is replaced by chlorite. Also, there is the presence of disseminated secondary minerals such as sulfides (pyrites) and of quartz veinlets in hand specimens. The latter mineral assemblage is similar in composition but not in intensity to the hydrothermal alteration mineral assemblage at the Obuasi mines, which are located about 30 km south of the crater structure (Appiah 1991 and Yao and Robb 2000).

Further evidence of hydrothermal alteration is based on a) visual description of samples (presence of disseminated sulphides, bleached samples and quartz veinlets) and b) thin-section petrography (plagioclase strongly sericitized and biotite replaced by chlorite). Some of the alteration occurs along foliation planes, in fractures, and in pore spaces caused by brittle-ductile deformation. The presence of some of these alteration minerals (e.g., sulfides and sericite) in some of the country rock fragments in the suevite suggests that the alteration is pre-impact.

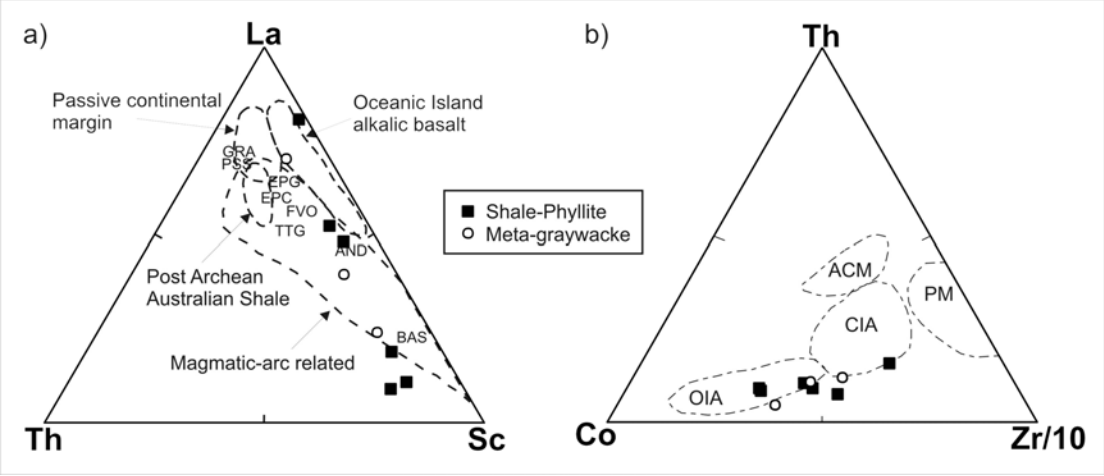

Fig. 15. a) La-Th-Sc ternary plots with fields defined by Girty and Barber (1993). Source rock compositions are for Early Proterozoic volcanic rocks (basalts [BAS], andesites [AND], and felsic volcanic rocks [FVO]); Proterozoic tonalite-trondhjemite-granodiorite (TTG); Early Proterozoic crust (EPC); Early Proterozoic graywackes (EPG); Proterozoic sandstones (PSS); Proterozoic granites (GRA), (Condie 1993). b) Co-Th-Zr diagram for tectonic setting discrimination (after Bhatia and Crook 1986). Oceanic island arc (OIA); continental island arc (CIA); active continental margin (ACM); passive margin (PM).

Post-Impact Alteration

Impact cratering is a high-energy, dynamic event that results in shock-metamorphic effects due to very high pressure and temperature. This leads to the irreversible deformation of the crystal structure of minerals, as well as to the formation of high-pressure polymorphs. On the basis of the presence of melt/glass, diaplectic quartz glass, multiple sets of PDFs, and lechatelierite clasts in Bosumtwi fallout suevite, Boamah and Koeberl (2006) estimated the maximum shock pressure experienced by the country rocks to be about 60 GPa. According to, for example, Koeberl and Reimold (2004, and references therein), the transient, high-energy, high-temperature impact event can also activate hydrothermal systems within and even outside of the crater.

There is evidence of post-impact alteration in the suevite samples of the Bosumtwi structure, as indicated by argillic alteration of melt particles and fine-grained clasts in the matrix to phyllosilicates. Alteration in the form of fractures filled with iron oxides has also been observed in suevite, e.g., sample LB-39A. This alteration of suevite, unlike the pre-impact alteration of country rocks that is associated with shear zones and gold mineralization, is not related to shearing.

Geochemistry of Bosumtwi Country Rocks in Comparison with Published Data for Birimian Rocks

The country rocks, melt fragments from suevites, and bulk suevites have elevated values of Fe_2O_3, Co, Cr, and V compared to average upper continental crust (Table 4). The suevites have average Co, Cr, and V contents of 21.6 (±4.3), 134 (±28), and 122 (±27) ppm, respectively, and the melt fragments from suevites have average Co, Cr, and V contents of 23.2 (±4.0), 134 (±43), and 98 (±25) ppm, respectively. The granites also have average Co, Cr, and V contents of 12.4 (±7.8), 146 (±227), and 84 (±40) ppm, respectively. The shale-phyllites, on the other hand, have average Co, Cr, and V contents of 17 (±9), 106 (±31), and 121 (±15) ppm, respectively. These average Co, Cr, and V contents of the target rocks, melt fragments from suevite and bulk suevites are similar to, and, in some cases lower than, the background values reported for Birimian meta-graywackes and metapelites by Asiedu et al. (2004).

Asiedu et al. (2004) analyzed 24 relatively fresh samples, comprising 19 meta-graywacke and 5 metapelites (gray and black phyllites and schist), for their major and trace elements contents. The location of these samples is about 50 km southeast of the crater and located within the Cape Coast Basin, with coordinates defined by longitudes 0°46′W to 0°54′W and latitudes 5°54′N to 6°04′N. The Birimian Supergroup in the area is mainly composed of metasedimentary rocks comprising meta-graywackes with subordinate quartzites and interbedded metapelites (gray and black phyllites and schist) (Asiedu et al. 2004).

Averages and ranges of siderophile and chalcophile element (Fe_2O_3, Cr, Co, and V) contents of these meta-graywacke and metapelite samples were calculated from the reported data (see Table 5).

The elevated values obtained in this study for the siderophile elements in country rocks and suevites, compared to average upper continental crust values, therefore, do not indicate the presence of an extraterrestrial component in the suevite, because the Birimian rocks already had elevated contents of these elements. Pyrite, chalcopyrite, and pyrrhotite are just some of the sulfides occurring in significant amounts in the country rocks. The only indication for a possible meteoritic component could be the small excess in Ni

and Co in melt fragments from suevites, as in similar glassy fragments Koeberl and Shirey (1993) detected a very small meteoritical component from Os isotope ratios.

The meta-graywacke samples of this study and those of Dai et al. (2005) also have low SiO_2/Al_2O_3 ratios, which is indicative of their immaturity (Asiedu et al. 2004) and that the sediments of the meta-graywacke might not have been transported far from their source.

The analyzed granite samples from Bosumtwi generally belong to the Belt-type (Dixcove) granitoids. This is based on the classification parameters of Leube et al. (1990), which indicate that the Belt-type rocks have higher Na_2O and CaO contents and lower K_2O and Rb contents than the Basin-type rocks. The lower CaO contents of the analyzed samples compared to those obtained by Leube et al. (1990) may be attributed to alteration in the analyzed samples. The total alkali element abundance ($Na_2O + K_2O$ versus silica) diagram (Fig. 11) after Cox et al. (1979) shows that most of the Bosumtwi granites are clearly Belt-type granitoids; further, their dioritic to quartz-dioritic composition compares favorably with the Belt-type granites described by Hirdes et al. (1992).

SUMMARY AND CONCLUSIONS

We describe some petrographic and geochemical characteristics of the country rocks and suevites at Bosumtwi crater and try to constrain the various phases of alteration that are believed to have affected the country rocks, namely: a) pre-impact hydrothermal alteration associated with gold mineralization and the formation of hydrothermal alteration halos along the contacts between metasediments and metavolcanics (Leube et al. 1990), and b) the much more localized post-impact alteration associated with the impact cratering. The following conclusions can be drawn from our studies:

1. The Birimian country rocks in the area around the Bosumtwi impact structure are characterized by pre-impact alteration associated with shearing. This is indicated by the abundance of hydrous minerals such as chlorite, sericite, sphene, quartz, and sulfides, which tend to fill the pore space between primary minerals. Some of these secondary minerals also replace the pre-existing metamorphic minerals, for example, sericite after plagioclase. There is also post-impact alteration, which is characterized by argillic alteration of glass and melt particles to phyllosilicate minerals; this post-impact alteration is not associated with shearing.
2. Optical microscopy revealed shock metamorphic effects in mineral and rock clasts of suevite samples, such as the presence of melt clasts, diaplectic quartz glass, ballen quartz, and a few quartz grains with PDFs. There is no evidence of shock metamorphism in the studied country rocks.
3. The elevated siderophile element contents of suevites and country rocks are attributed to the sulfide minerals associated with the Birimian hydrothermal alteration and do not indicate the presence of an extraterrestrial component in the suevite samples.
4. The granites of the country rocks have tonalitic to quartz-dioritic composition and, on the basis of trace element discrimination plots, are of volcanic-arc tectonic provenance. The provenance studies have indicated that the Bosumtwi metasediments are volcanic-arc related. This supports the view of Leube et al. (1990), indicating that the metasedimentary and the metavolcanic units were formed contemporaneously.

Acknowledgments–The authors thank the Austrian Exchange Service (ÖAD) for providing a Ph.D. scholarship to F. Karikari. This work was supported by the Austrian FWF (grant P17194-N10 to C. K.) and by a grant of the Austrian Academy of Sciences (to C. K.). We are grateful to the Geological Survey of Ghana for logistical support and to K. Atta-Ntim (GSD, Kumasi, Ghana) and D. Brandt (then University of the Witwatersrand, Johannesburg) for help in the field in 1997. We appreciate the help of H. Böck, M. Villa, M. Bichler, and G. Steinhauser (Atominstitut Vienna) with the irradiations. We are grateful to J. Morrow (San Diego State University) and an anonymous reviewer for very helpful reviews and extensive comments on this manuscript.

Editorial Handling—Dr. Bernd Milkereit

REFERENCES

Appiah H. 1991. Geology and mine exploration trends of Prestea Goldfields, Ghana. *Journal of African Earth Science* 13:235–241.

Asiedu D. K., Dampare S. B., Asamoah-Sakyi P., Banoueng-Yakubo B., Osae S., Nyarko B. J. B., and Manu J. 2004. Geochemistry of Paleoproterozoic metasedimentary rocks from the Birim diamondiferous field, southern Ghana: Implications for provenance and crustal evolution at the Archean-Proterozoic boundary. *Geochemical Journal* 38:215–228.

Bhatia M. R. and Crook K. A. W. 1986. Trace element characteristics of greywackes and tectonic setting discrimination of sedimentary basins. *Contributions to Mineralogy and Petrology* 92:181–193.

Boamah D. 2001. Bosumtwi impact structure, Ghana: Petrography and geochemistry of target rocks and impactites, with emphasis on shallow drilling project around the crater. Ph.D. thesis, University of Vienna, Vienna, Austria.

Boamah D. and Koeberl C. 2002. Geochemistry of soils from the Bosumtwi impact structure, Ghana, and relationship to radiometric airborne geophysical data. In *Meteorite impacts in Precambrian shields*, edited by Plado J. and Pesonen L. Impact Studies, vol. 2. Heidelberg: Springer. pp. 211–255.

Boamah D. and Koeberl C. 2003. Geology and geochemistry of shallow drill cores from the Bosumtwi impact structure, Ghana. *Meteoritics & Planetary Science* 38:1137–1159.

Boamah D. and Koeberl C. 2006. Petrographic studies of fallout suevite from outside the Bosumtwi impact structure, Ghana. *Meteoritics & Planetary Science* 41:1761–1774.

Chao E. C. T. 1968. Pressure and temperature histories of impact metamorphosed rocks-based on petrographic observations. In *Shock metamorphism of natural materials*, edited by French B. M. and Short N. M. Baltimore, Maryland: Mono Book Corp. pp. 135–158.

Condie K. C. 1993. Chemical composition and evolution of the upper continental crust: Contrasting results from surface samples and shales. *Chemical Geology* 104:1–37.

Cox K. G., Bell J. D., and Pankhurst R. J. 1979. *The interpretation of igneous rocks.* London: Allen & Unwin. 450 p.

Dai X., Boamah D., Koeberl C., Reimold W. U., Irvine G., and McDonald I. 2005. Bosumtwi impact structure, Ghana: Geochemistry of impactites and target rocks, and search for a meteoritic component. *Meteoritics & Planetary Science* 40: 1493–1511.

Dickinson W. R. and Suczek C. A. 1979. Plate tectonics and sandstone compositions. *The American Association of Petroleum Geologists Bulletin* 63:2164–2182.

Dickinson W. R., Beard L. S., Brakenridge G. R., Erjavec J. L., Ferguson R. C., Inman K. F., Knepp R., Lindberg F. A., and Ryberg P. T. 1983. Provenance of North American Phanerozoic sandstones in relation to tectonic setting. *Geological Society of America Bulletin* 94:222–235.

Dzigbodi-Adjimah K. 1993. Geology and geochemical patterns of the Birimian gold deposits, Ghana, West Africa. *Journal of Geochemical Exploration* 47:305–320.

Earth Impact Database, 2006. http://www.unb.ca/passc/ImpactDatabase. Accessed 08 October 2006.

El Goresy A. 1966. Metallic spherules in Bosumtwi crater glasses. *Earth and Planetary Science Letters* 1:23–24.

El Goresy A., Fechtig H., and Ottemann T. 1968. The opaque minerals in impactite glasses. In *Shock metamorphism of natural materials*, edited by French B. M. and Short N. M. Baltimore, Maryland: Mono Book Corp. pp. 531–554.

Eisenlohr B. N. and Hirdes W. 1992. The structural development of the early Proterozoic Birimian and Tarkwaian rocks of southwest Ghana, West Africa. *Journal of African Earth Sciences* 14:313–325.

Feybesse J., Billa M., Guerrot C., Duguey E., Lescuyer J., Milesi J., and Bouchot V. 2006. The paleoproterozoic Ghanaian province: Geodynamic model and ore controls, including regional stress modeling. *Precambrian Research* 149:149–196.

Gentner W., Lippolt H. J., and Müller O. 1964. The potassium-argon age of the Bosumtwi crater in Ghana and the chemical composition of its glasses. *Zeitschrift für Naturforschung* 19A: 150–153.

Girty G. H. and Barber R. W. 1993. REE, Th, and Sc evidence for the depositional setting and source rock characteristics of the Quartz Hill chert, Sierra Nevada, California. In *Processes controlling the composition of clastic sediments*, edited by Johnsson M. J. and Basu A. GSA Special Paper #284. Boulder, Colorado: Geological Society of America. pp.109–119.

Herron M. M. 1988. Geochemical classification of terrigenous sands and shales from core or log data. *Journal of Sedimentary Petrology* 58:820–829.

Hirdes W., Davis D. W., and Eisenlohr B. N. 1992. Reassessment of Proterozoic granitoid ages in Ghana on the basis U/Pb zircon and monazite dating. *Precambrian Research* 56:89–96.

Hirdes W., Davis D. W., Lüdtke G., and Konan G. 1996. Two generations of Birimian (Paleoproterozoic) volcanic belts in northeastern Côte d'Ivoire (West Africa): Consequences for the "Birimian controversy." *Precambrian Research* 80:173–191.

John T., Klemd R., Hirdes W., and Loh G. 1999. The metamorphic evolution of the Paleoproterozoic (Birimian) volcanic Ashanti belt (Ghana, West Africa). *Precambrian Research* 98:11–30.

Jones W. B. 1985. Chemical analyses of Bosumtwi crater target rocks compared with the Ivory Coast tektites. *Geochimica et Cosmochimica Acta* 48:2569–2576.

Jones W. B., Bacon M., and Hastings D. A. 1981. The Lake Bosumtwi impact crater, Ghana. *Geological Society of America Bulletin* 92:342–349.

Junner N. R. 1937. The geology of the Bosumtwi caldera and surrounding country. *Gold Coast Geological Survey Bulletin* 8: 1–38.

Karp T., Milkereit B., Janle J., Danour S. K., Pohl J., Berckhemer H., and Scholz C. A. 2002. Seismic investigation of the Lake Bosumtwi impact crater: Preliminary results. *Planetary and Space Science* 50:735–743.

Koeberl C. 1993. Instrumental neutron activation analysis of geochemical and cosmochemical samples: A fast and proven method for small samples analysis. *Journal of Radioanalytical and Nuclear Chemistry* 168:47–60.

Koeberl C. and Reimold W. U. 2004. Post-impact hydrothermal activity in meteorite impact craters and potential opportunities for life. In *Bioastronomy 2002: Life among the stars*, edited by Norris R. P. and Stootman F. H. San Francisco: Astronomical Society of the Pacific. pp. 299–304.

Koeberl C. and Reimold W. U. 2005. Bosumtwi impact crater, Ghana (West Africa): An updated and revised geological map, with explanations. *Jahrbuch der Geologischen Bundesanstalt, Wien (Yearbook of the Austrian Geological Survey)* 145:31–70 (+1 map, 1:50,000).

Koeberl C. and Shirey S. B. 1993. Detection of a meteoritic component in Ivory Coast tektites with rhenium-osmium isotopes. *Science* 261:595–598.

Koeberl C., Bottomley R. J., Glass B. P., and Storzer D. 1997. Geochemistry and age of Ivory Coast tektites and microtektites. *Geochimica et Cosmochimica Acta* 61:1745–1772.

Koeberl C., Reimold W. U., Blum J. D., and Chamberlain C. P. 1998. Petrology and geochemistry of target rocks from the Bosumtwi impact structure, Ghana, and comparison with Ivory Coast tektites. *Geochimica et Cosmochimica Acta* 62:2179–2196.

Leube A., Hirdes W., Maur R., and Kesse G. O. 1990. The early Proterozoic Birimian Supergroup of Ghana and some aspects of its associated gold mineralization. *Precambrian Research* 46: 139–165.

Littler J., Fahey J. J., Dietz R. S., and Chao E. C. T. 1961. Coesite from the Lake Bosumtwi crater, Ashanti, Ghana (abstract). GSA Special Paper #68. Boulder, Colorado: Geological Society of America. 218 p.

Mader D. and Neubauer F. 2004. Provenance of Palaeozoic sandstones from the Carnic Alps (Austria): Petrographic and geochemical indicators. *International Journal of Earth Science* 93:262–281.

Manu J. 1993. Gold deposits of Birimian greenstone belt in Ghana: Hydrothermal alteration and thermodynamics. Ph.D. thesis, Braunschweiger Geologisch–Paläontologische Dissertationen vol. 17, Braunschweig, Germany.

Melcher F. and Stumpfl E. F. 1994. Palaeoproterozoic exhalite formation in northern Ghana: Source of epigenetic gold-quartz vein mineralization? *Geologisches Jahrbuch* 100:201–246.

Milesi J. P., Ledru P., Feybesse J. L., Dommanget A., and Macoux E. 1992. Early Proterozoic ore deposits and tectonics of the Birimian orogenic belt, West Africa. *Precambrian Research* 58: 305–344.

Moon P. A. and Mason D. 1967. The geology of 1/4° field sheets 129 and 131, Bompata S.W. and N.W. *Ghana Geological Survey Bulletin* 31:1–51.

Oberthür T., Vetter U., Schmit-Mumm A., Weiser T., Amanor J. A.,

Gyapong J. A., Kumi R., and Blenkinsop T. G. 1994. The Ashanti gold mine at Obuasi, Ghana: Mineralogical, geochemical, stable isotope and fluid inclusion studies on the metallogenesis of the deposit. *Geologisches Jahrbuch* D100: 31–129.

Okada H. 1971. Classification of sandstones: Analysis and proposals. *Journal of Geology* 79:509–525.

Osae S., Asiedu D. K., Banoeng-Yakubo B., Koeberl C., and Dampare S. B. 2006. Provenance and tectonic setting of late Proterozoic Buem Sandstones of southern Ghana: Evidence from geochemistry and detrital modes. *Journal of African Earth Sciences* 44:85–96.

Pearce J. A., Harris N. B. W., and Tindle A. G. 1984. Trace element discrimination diagrams for the tectonic interpretation of granitic rocks. *Journal of Petrology* 25:956–983.

Pelig-Ba K. B., Parker A., and Price M. 2004. Trace element geochemistry from the Birimian metasediments of the northern region of Ghana. *Water, Air, and Soil Pollution* 153:69–93.

Pesonen L. J., Koeberl C., and Hautaniemi H. 1998. Aerogeophysical studies of the Bosumtwi impact structure. *GSA Abstracts with Programs* 30:A190.

Pettijohn F. J., Potter P. E., and Siever R. 1972. *Sand and sandstone.* Berlin-Heidelberg-New York: Springer. 618 p.

Reimold W. U., Brandt D., and Koeberl C. 1998. Detailed structural analysis of the rim of a large, complex impact crater: Bosumtwi crater, Ghana. *Geology* 26:543–546.

Reimold W. U., Koeberl C., and Bishop J. 1994. Roter Kamm impact crater, Namibia: Geochemistry of basement rocks and breccias. *Geochimica et Cosmochimica Acta* 58:2689–2710.

Rollinson R. H. 1993. *Using geochemical data: Evaluation, presentation, interpretation.* Harlow, Essex: Longman Group UK Limited. 347 p.

Rosenberg P. E. 1967. Subsolidus relations in the system $CaCO_3$-$MgCO_3$-$FeCO_3$ between 350 and 550 °C. *American Mineralogist* 52:787–796.

Scholz A. C., Karp T., Brooks M. K., Milkereit B., Amoako P. Y. O., and Arko A. J. 2002. Pronounce central uplift identified in the Bosumtwi impact structure, Ghana, using multichannel seismic reflection data. *Geology* 30:939–942.

Sylvester P. J. and Attoh K. 1992. Lithostratigraphy and composition of 2.1 Ga greenstone belts of the West African Craton and their bearing on crustal evolution and the Archean-Proterozoic boundary. *Journal of Geology* 100:377–393.

Taylor P. N., Moorbath S., Leube A., and Hirdes W. 1992. Early Proterozoic crustal evolution in the Birimian of Ghana: Constraints from geochronology and isotope geochemistry. *Precambrian Research* 56:97–111.

Taylor S. R. and McLennan S. M. 1985. *The continental crust: Its composition and evolution.* Oxford: Blackwell Scientific Publications. 312 p.

Woodfield P. D. 1966. The geology of the 1/4° field sheet 91, Fumso, N.W. Ghana. *Ghana Geological Survey Bulletin* 30:1–66.

Wright J. B., Hastings D. A., Jones W. B., and Williams H. R. 1985. *Geology and mineral resources of West Africa.* London: Allen & Unwin. 165p.

Yao Y. and Robb L. J. 2000. Gold mineralization in Palaeoproterozoic granitoids at Obuasi, Ashanti region, Ghana: Ore geology, geochemistry and fluid characteristics. *South African Journal of Geology* 103:255–278.